Meteorological Significance of Cloud Tracked Winds During DST-5 and DST-6

H. Michael Goodman
Frederick Mosher
Tod Stewart
Verner Suomi

July 1981

Space Science and Engineering Center
University of Wisconsin
1225 West Dayton St.
Madison, Wisconsin 53706

Abstract

A study has been conducted to determine the meteorological significance of satellite derived cloud drift winds using data from the Data Systems Test (DST). Three synoptic weather events were chosen during DST-6 (January 5 - March 5) for weather analysis and comparison. The three events each contained a prominent weather feature over the north Pacific Ocean. Two satellite sources (NESS and the University of Wisconsin), radiosonde and commercial aircraft reports combined to produce a wind set covering the target area.

The radiosonde data were primarily limited to Alaska and the west coasts of the United States and Canada. As a result the radiosonde reports produced excellent analyses over the land regions but failed miserably over the oceanic regions. The commercial aircraft observations were restricted to the upper levels and, therefore, could not provide any data below 300 mb. However, the upper level aircraft analyses were spatially complete and provided an accurate description of the wind field. The University of Wisconsin Space Science and Engineering Center (UW/SSEC) provided satellite cloud drift winds for analysis. The SSEC wind set produced the greatest number of wind observations of all the data sources, but they were restricted to cloud covered regions. The satellite winds were also limited to latitudes south of 50°N. The SSEC wind field analyses were generally consistent and provided a sound upper and lower level analysis. The fourth data source was the NESS satellite winds. They, too, were restricted to cloud environments, but in addition they suffered from a lack of sufficient wind vectors. Those vectors which were produced were accurate but were not sufficient to stand alone. When all four data sources

were combined they produced a meteorologically consistent data analysis which reflected the movement and development of the extra-tropical cyclones and anticyclones through the DST area.

1. Introduction

Satellites offer a valuable means for obtaining weather observations in data poor regions of the world. In addition, they can enhance and compliment standard forms of meteorological measurements obtained over land. Satellite soundings have been studied and examined extensively by the National Meteorological Center (NMC) and the National Aeronautics and Space Agency/Goddard Institute of Space Studies (NASA/GISS). However, satellite derived cloud winds have not received as much attention. The impact of satellite cloud winds upon the description of meteorologically significant features is the primary focus of this report. Once the validity and accuracy of satellite winds have been ascertained, assimilation into forecast models may prove feasible and productive.

The Space Science and Engineering Center (SSEC) at the University of Wisconsin-Madison participated in two Data Systems Test (DST) programs. DST-5 was conducted between August 16 and September 12, 1975. While DST-6 covered the period between January 5, and March 5, 1976. Several sources of data were available for study within these time periods. Data analysis was performed on the NMC Level III wind field, and the level II wind fields produced by SSEC cloud tracking, National Environmental Satellite Service (NESS) cloud tracking, aircraft and radiosonde winds.

The SSEC satellite tracked winds were gathered through the use of McIDAS (Man-computer Interactive Data Access System). McIDAS is an image storage, display and processing system consisting of data archive, data access, video display, operator console and computer control sections (Chatters and Suomi, 1975). Visible and infrared (IR) satellite images are transmitted directly to the SSEC building and are received by antenna stationed on the roof. The data may be archived or used on a real time

basis. To obtain cloud drift winds from satellite observations an accurate technique for tracking and determining cloud heights must be employed. At SSEC this is possible through special McIDAS hardware and software which allows the operator to loop, enhance, magnify and superimpose a series of satellite images on a television screen.

Cloud tracking can be done by one of two possible methods. The first is cursor tracking of a cloud to the nearest TV line and element (pixel tracking). The operator positions a cursor over a cloud feature and follows its movement through a series of satellite images. The displacement of the cloud feature between satellite images produces the cloud motion vector. Single pixel tracking can be used for tracking multi-layer flow patterns of for matching the motion of the cursor to the motion of a pattern of clouds.

Correlation tracking is the second method used in cloud tracking. Correlation tracking requires the operator to place a cloud within a cursor outlined box and track its movement through a satellite picture sequence. The computer performs a correlation analysis to align to brightness fields within the cursor and "fine tune" the operators tracking. Correlation tracking is more accurate than single pixel tracking but it requires well defined clouds moving in a single flow layer (Mosher, 1975).

Cloud height determination is extremely important in cloud tracking. The wind field cannot be described accurately without the knowledge of the height of the clouds being tracked. Cloud height determination employs both visible and infrared images. The visible data is used to determine the emissivity of the cloud. Once the emissivity is known, the infrared black body temperature may then be adjusted to obtain the cloud top temperature. During DST-5 comparisons of cloud top temperatures with standard atmospheric

sounding, corrected for latitude and date, yielded the approximate cloud height. If the visible data was not available then the black body temperature of the cloud was used. The cloud height may be calculated automatically or independently of the wind calculation.

Cloud height determinations during DST-6 were somewhat different than previous DST events. Analysis of previous DST data sets indicated cloud height errors of up to 100 mb. The cause of the large errors were a result of the use of corrected climatic soundings rather than actual synoptic soundings. SSEC at the University of Wisconsin was not equipped to receive world wide synoptic sounding coverage. Therefore, SSEC sent GISS cloud top temperature and cloud thickness information. GISS then performed the conversions of the cloud temperature and thickness into cloud heights and transmitted the information back to SSEC. GISS used the most current global analysis for the conversions. Generally the synoptic soundings available were within 18-24 hours of the wind vector observation. Once the cloud height and thickness were known the wind levels could be assigned to a data set. There have been very few in situ experiments on wind levels within cloud formations. Therefore, a set procedure was used to assign a level to the cloud motion vectors. If the base of the cloud was below 850 mb then the wind was placed at the bottom of the cloud. If the cloud base was below 950 mb then the resultant wind was placed at 950 mb. If the cloud top was above 300 mb, then the wind vector was assigned to the cloud top. Any clouds with bases above 850 mb and tops below 300 mb had their wind vectors placed in the middle of the cloud. Errors in cloud top temperature or errors with the satellite soundings resulted in the placement of some wind vectors in the stratosphere. These clouds were probably located at or near the tropopause.

This was not corrected during the DST due to the extensive software development required.

The satellite derived wind measurements used a three image loop sequence to compute the cloud motion vectors. To achieve quality control the same cloud motion measurements were taken twice using the two picture pairs. Those wind computations which did not agree within 5 ms-1 for either the u or v components or differed by more than 100 mb in the Z component were flagged and removed from the data set. However, there were times when one of the images was unusable. In these instances only one picture pair could be used. Quality control was then placed in the hands of the operator. It became the operators responsibility to perform the quality check.

NESS provided the other source of satellite wind measurements. The NESS wind vectors were obtained from time-lapse movie loops. The loop include six images, of either visible or infrared pictures, taken over a 2 1/2 hour time span. The loop is run through a projector continously displaying the cloud motions. The movie loops were composed of 48 frames. The start and end images were repeated 20 times each, while the four internal images were each repeated twice. This allowed a pause in the loop at both the beginning and end of the sequence. The pause at both ends permitted cloud tracers to be indentified and their displacement to be measured. The loops were projected onto a plotting board where individual clouds were measured (Young, 1975).

Cloud height determinations were made via the infrared data. The IR image was displayed with 18 shades of gray representing cloud temperatures from 300 - 220K. Since black body temperatures were used to obtain cloud heights the cloud emissivity must be near unity. Therefore, the cloud tracers used must have a sufficient thickness to register an emissivity

between .75 and 1.0. Once the cloud top temperature, emissivity and surface temperatures are known a cloud height determination may be made.

In addition to satellite derived wind measurements, there were radiosonde and aircraft observations. The radiosonde coverage was primarily limited to land areas. Two exceptions are Hawaii and Ocean Station Papa located in the Gulf of Alaska. DST-6 which was centered over the Pacific Ocean (Figure 1) received information from radiosonde stations along the U. S. and Canadian west coast, including the Alaskan coast. Unlike satellite winds, radiosondes are not restricted to one or two levels. Radiosondes provide a continuous report of atmospheric conditions from the ground to the stratosphere. Radiosondes are generally considered to be ground truth although analysis based solely on radiosonde data would be inadequate and inaccurate (Young, 1975).

The fourth source of weather data came from commercial aircraft. The airlines generally fly between 10,500 - 13,000 meters on preselected routes over the Pacific Ocean. Therefore, the aircraft data, although quite good is somewhat limited in scope. The aircraft data was only used for the upper level analyses in the DST program.

The combination of all wind observation sources produced a more complete and accurate analysis of the synoptic situation. Analysis of individual and combined data sets is presented in Sections 3-5. The strength and weaknesses of these individual data sets are readily apparent in the analysis of the synoptic wind field.

2. DST Operations

DST-5 operated from August 16 - September 21, 1975. Wind sets were produced from cloud motions using SMS-1 image data. DST-5 was centered over the 75th meridian and covered both the northern and southern hemispheres.

Fig. 2. Approximate satellite coverage for DST-5

The areal coverage included most of North America and all of South America (Figure 2). Four wind sets were produced each day over the entire DST-5 period. There were some hardware failures which prevented some wind sets from being completed but nevertheless 95% of all possible wind sets were produced. Mosher (1975) gives a complete report on the operational aspect of the DST-5 program performed at SSEC of the University of Wisconsin-Madison.

DST-5 data was not completely analyzed and, therefore, will not be presented in this report. Problems arose with storage of data on computer tapes and slant track video tapes rendering a complete analysis of the data impossible. Despite this problem the SSEC participation in DST-5 proved to be extremely valuable in the design and preparation of the DST-6 wind sets (Mosher, 1975).

The Space Science and Engineering Center participated in DST-6 from January 5 through March 5, 1976. The areal coverage was centered on the 135th meridian and extended to 60° latitude both north and south. This region covered of the eastern and central Pacific Ocean. Four wind sets over this region were produced each 24 hour period by the SSEC cloud tracking team. A wind set consisted of three consecutive one half hour interval satellite images. The following time sequences were used to produce the four daily wind sets:

1. 2215GMT, 2245GMT, 2315GMT
2. 0345GMT, 0415GMT, 0445GMT
3. 0915GMT, 0945GMT, 1015GMT
4. 1445GMT, 1515GMT, 1545GMT

Every complete satellite image sequence produced two pairs images (i.e. 1st - 2nd image and 2nd - 3rd image). Cloud drift winds were tracked from T_1 to T_2 and from T_2 to T_3. During DST-6 it took 5 1/2 hours to

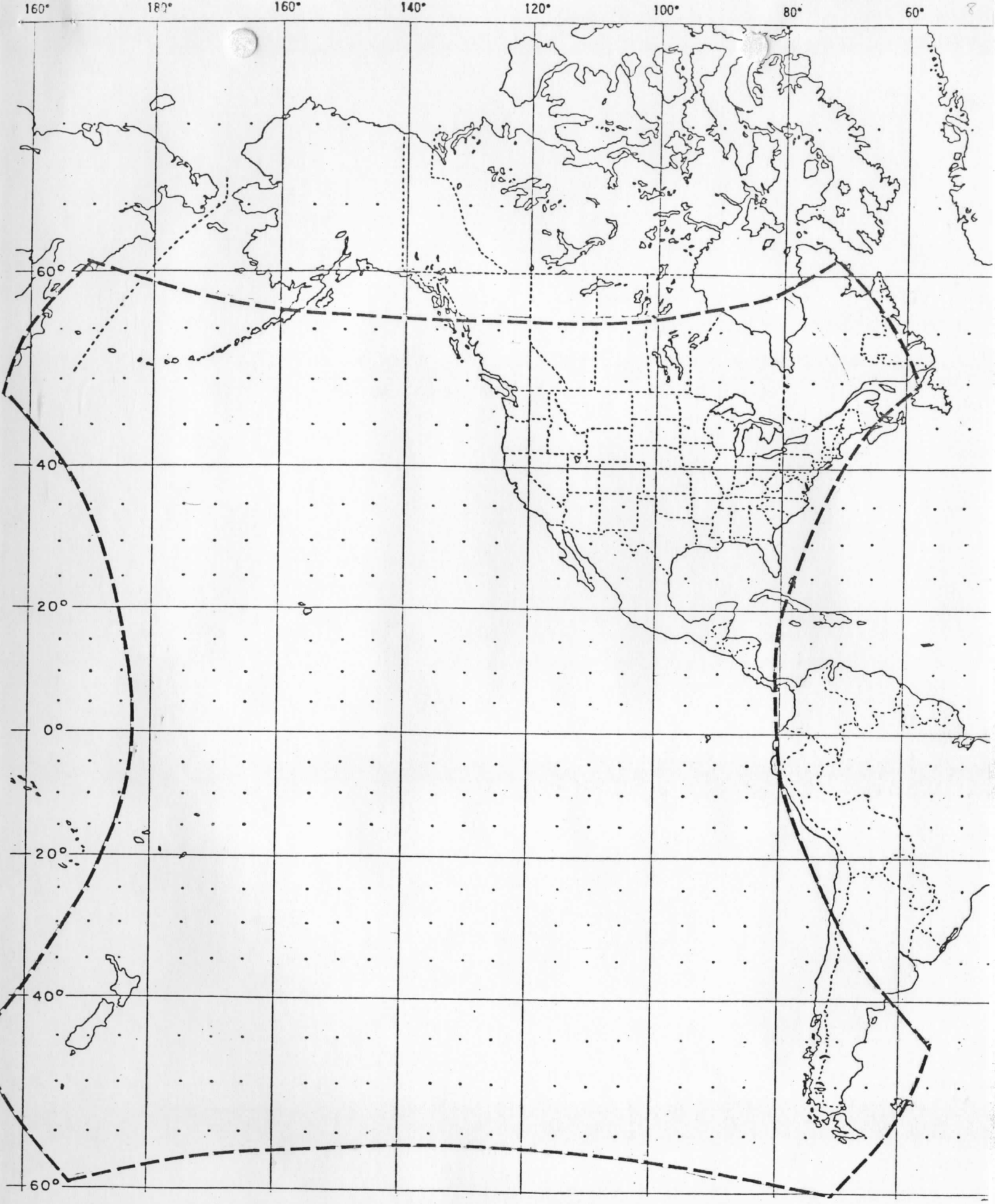

Fig. 1. Approximate satellite coverage for DST-6

complete a wind set. The five and one half hour time period can be broken down into 1 1/2 hours for the data ingest and another 4 hours to complete the actual data processing and cloud motion vectors. Cloud motion vectors were restricted to regions of cloud cover. In this experiment the imagery was limited to the visible and infrared spectrum (Mosher, 1976).

Although DST-6 covered a very large portion of the Pacific and continued 24 hours a day over a two month period, only a portion of the information was included in the actual data analysis. The analysis would become too large and cumbersome if the entire data set was used. The first restriction placed on the data was an areal one. A target area within the broad DST-6 data region was established. The target area was bounded by 110° - 180°W for the longitudinal boundaries and 20° - 70°N for the latitudinal boundaries. This area covered the west coast of North America to the east, Alaska to the north, the Bering Strait to the west and Hawaii to the south (Figure 3). Most of this region is over the Pacific Ocean where satellite data is needed for a synoptic analysis. In addition to areal restrictions, there were temporal restrictions placed on the DST-6 data. Sixty days of data could not be completely analyzed. Therefore, three time periods were chosen within the DST-6 framework for an in depth synoptic analysis. The three events occurred in the month of February. February 8-10 (Julian days 39-41), February 13-15 (Julian days 45-47) and finally February 25-27 (Julian days 56-58), 1976 were the times chosen. These three periods contained distinct meteorological features which could be analyzed by satellite derived wind vectors. Radiosonde and aircraft data were also available for these time periods. Together the satellite, radiosonde, and aircraft data were incorporated into a larger data set for synoptic analysis.

The analysis of the radiosonde, aircraft, NESS and SSEC data sets involved

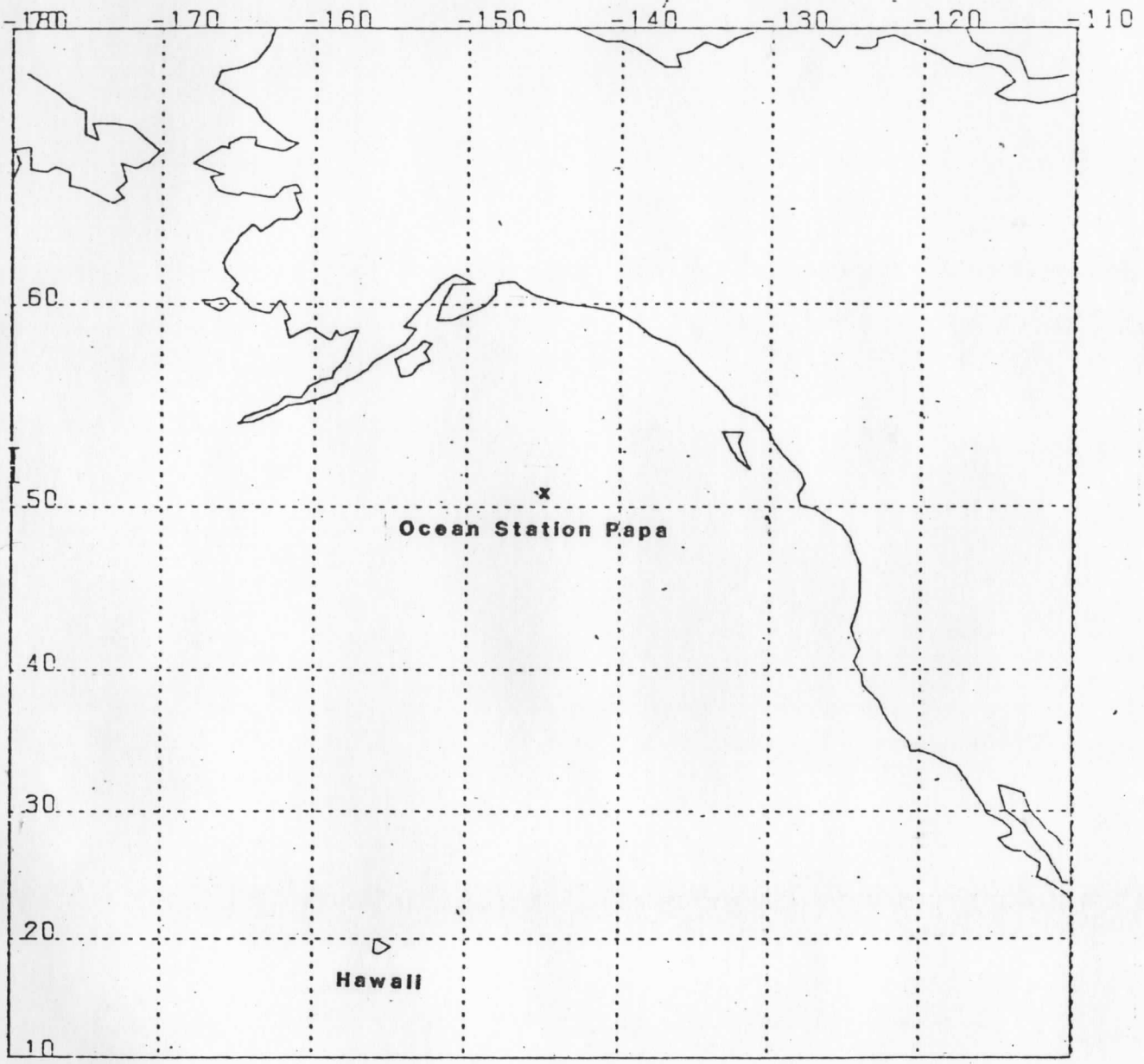

Fig. 3. Target area for DST-6

the computation and display of the streamlines, wind speeds, divergence and relative vorticity. The individual and combined data sets were used to complete the analysis. The data were classified and placed into low (999-651 mb), middle (650-351 mb) and upper (350-100 mb) levels. Figures 4-13 illustrate the density and location of the wind vectors obtained by the SSEC, NESS, radiosonde and aircraft observations. Each figure displays a standard wind set at one of the three height levels. Notice the higher density satellite upper and lower level winds as compared to the middle level wind vectors. The aircraft wind vectors are quite numerous, but limited to the upper level. A comparison of the satellite and aircraft winds with the radiosonde winds reveals the limitation of the first two sources in identifying northern cloud features. Only the radiosondes effectively cover the atmosphere over Alaska. Each level was analyzed and isopleths for the various meteorological quantities were produced via McIDAS. Analysis of the individual data sets indicated the importance of each data source towards producing an accurate description of the synoptic situation. However, just as important the analysis of the individual sets highlighted the inherent weakenesses and faults in a single data source.

3. Case I: February 7-10, 1976

The first synoptic event to be analyzed began on February 7, 1976 (38th Julian day). The Julian day reference for this day and succeeding days will be mentioned through out this report. The McIDAS analysis was performed on three different levels. Due to a lack of significant middle level (500 mb) observations, only the upper level (300 mb) and lower level (900 mb) will be presented with any detail. The 500 mb data set contained no aircraft observations. Radiosondes were only located along the boundary

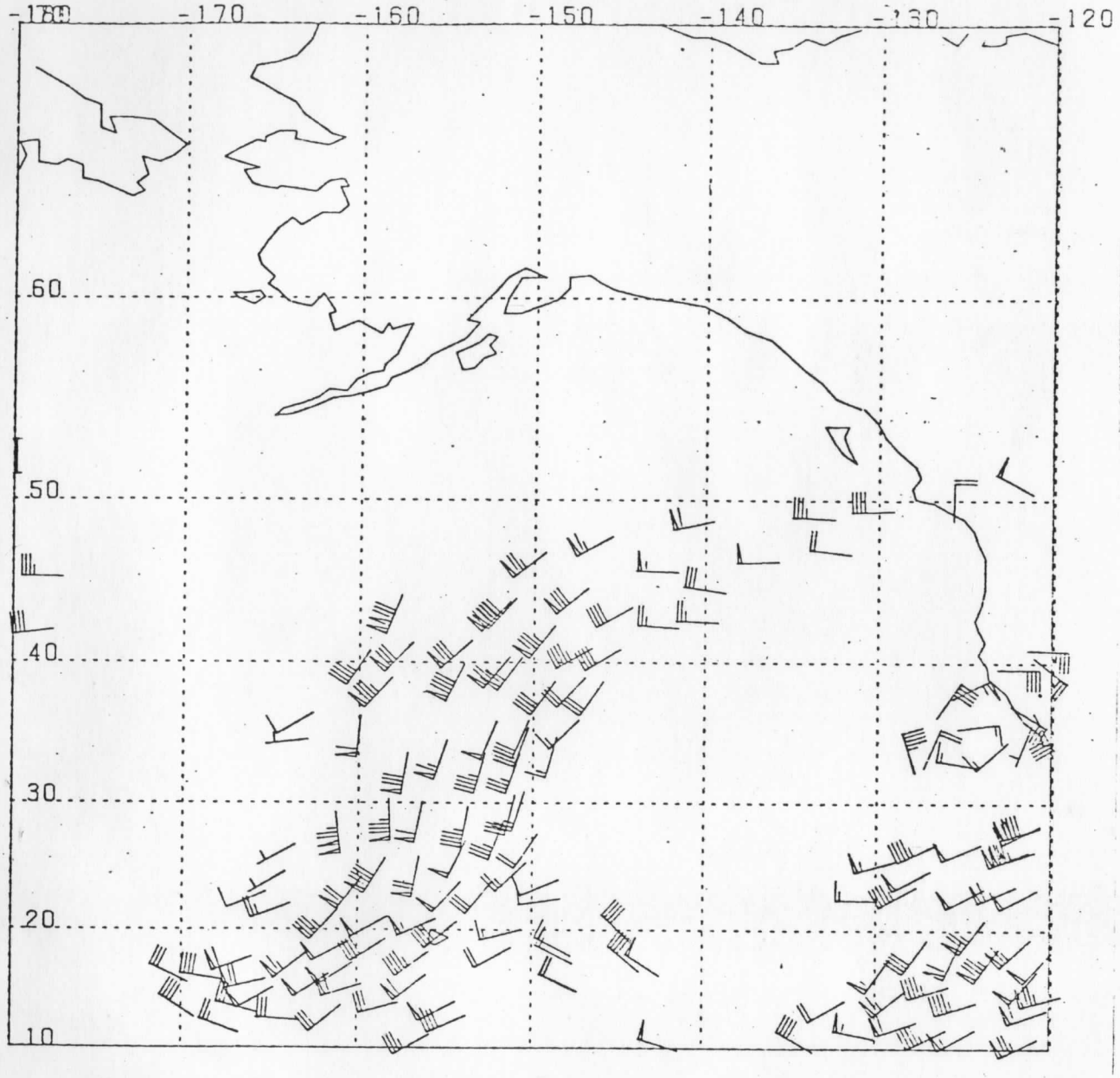

Fig. 4. High level SSEC winds for 7 February 1976

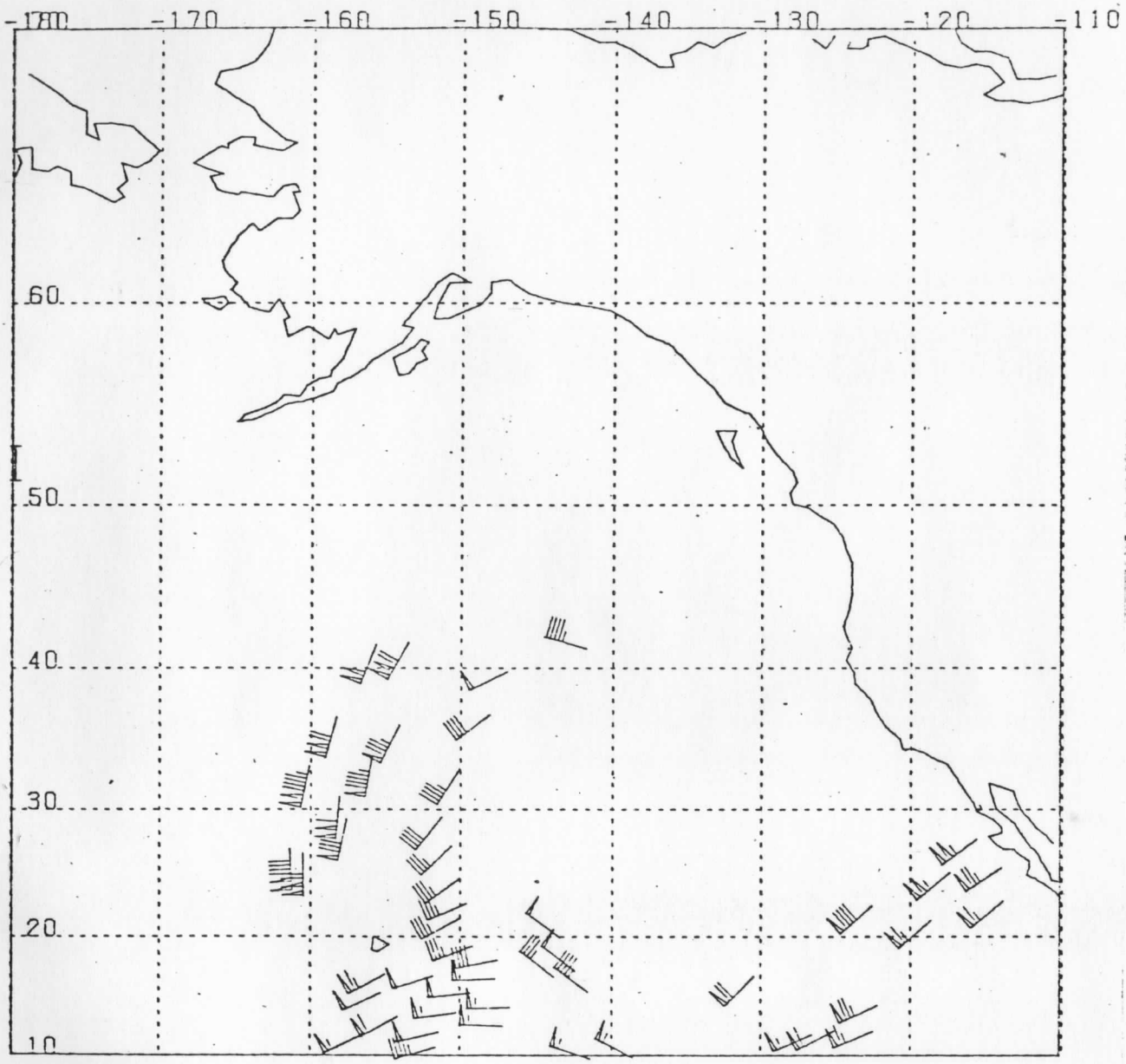

Fig. 5. High level NESS winds for 7 February 1976

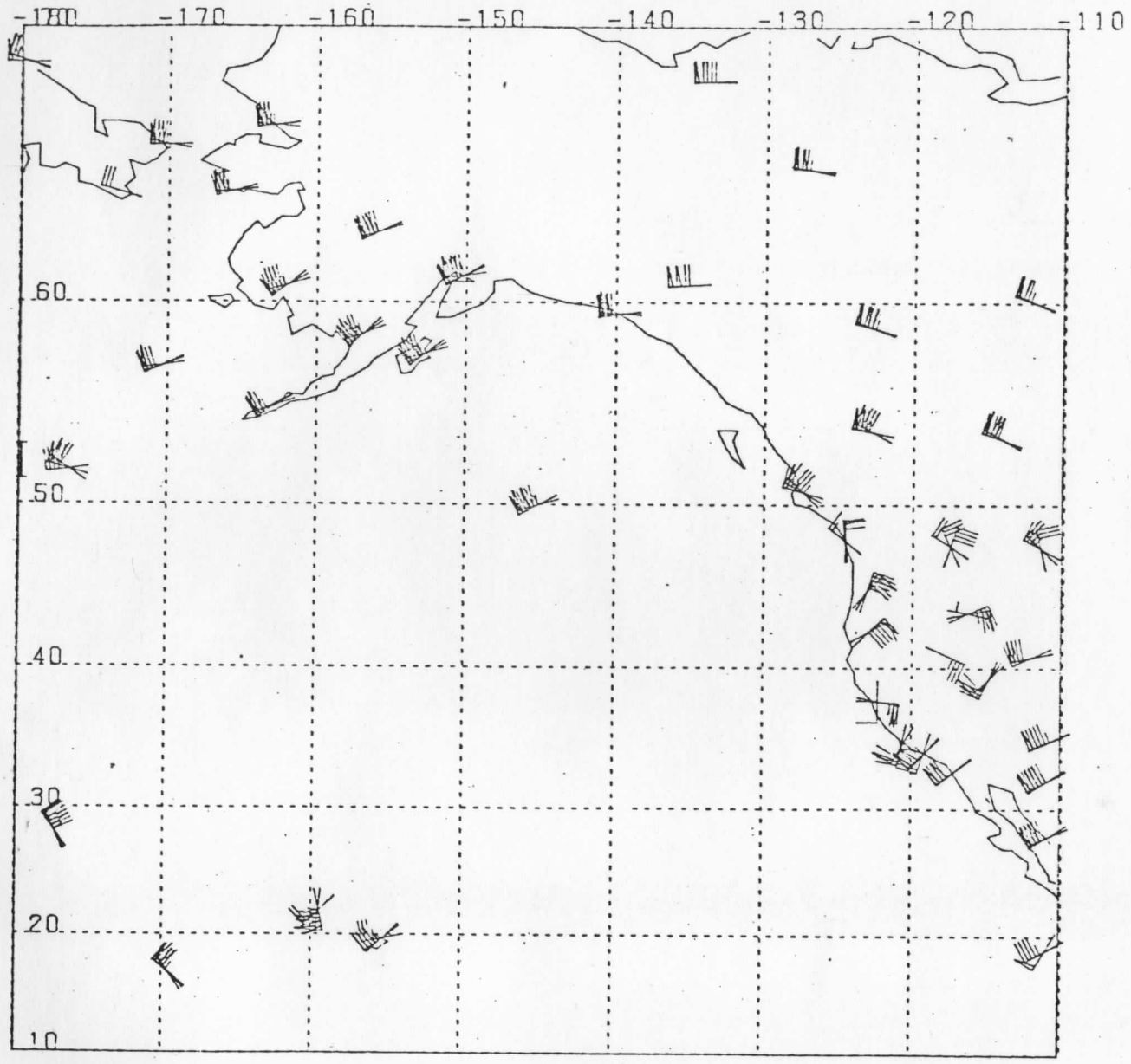

Fig. 6. High level Radiosonde winds for 7 February 1976

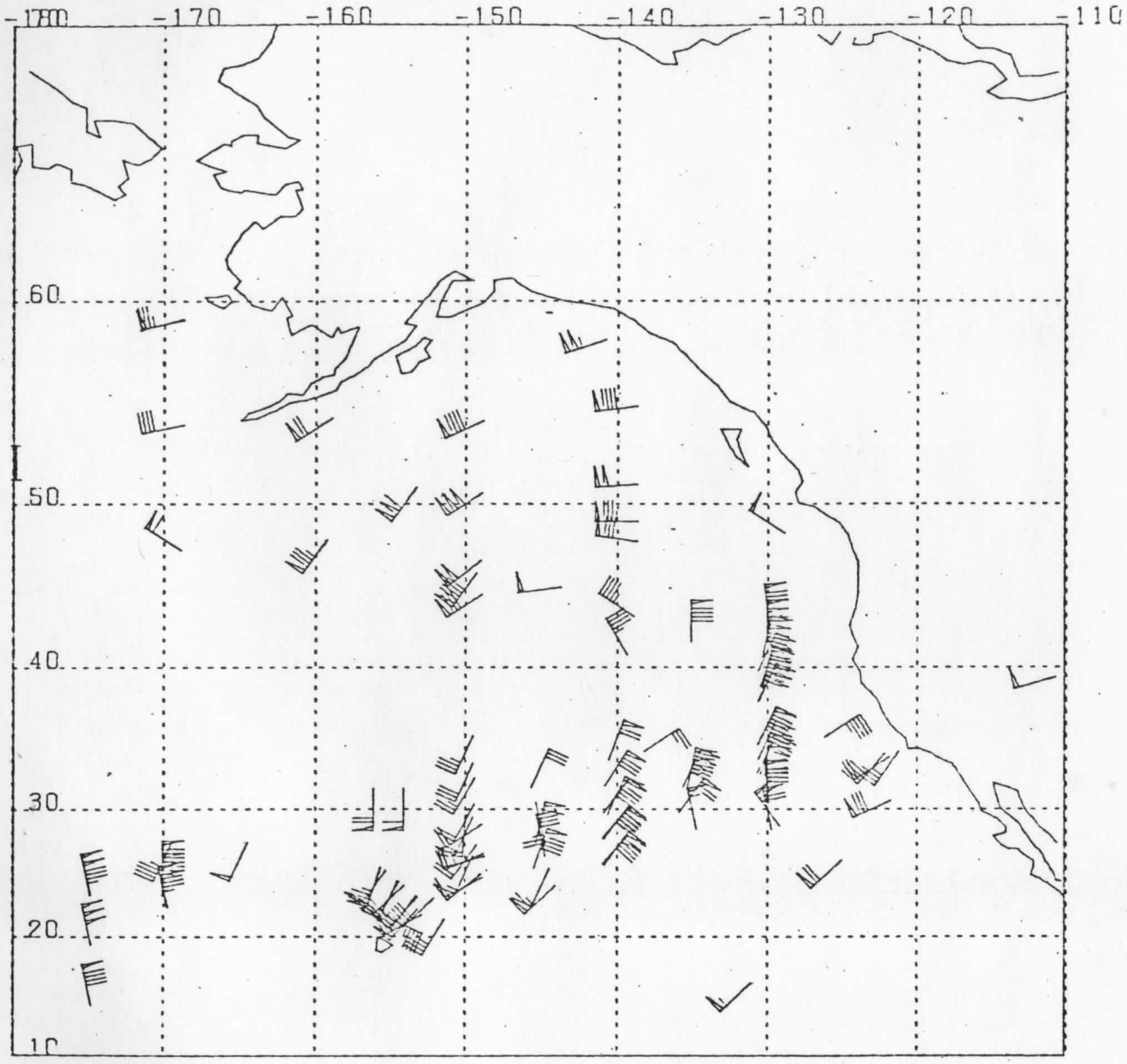

Fig. 7. High level Aircraft winds for 7 February 1976

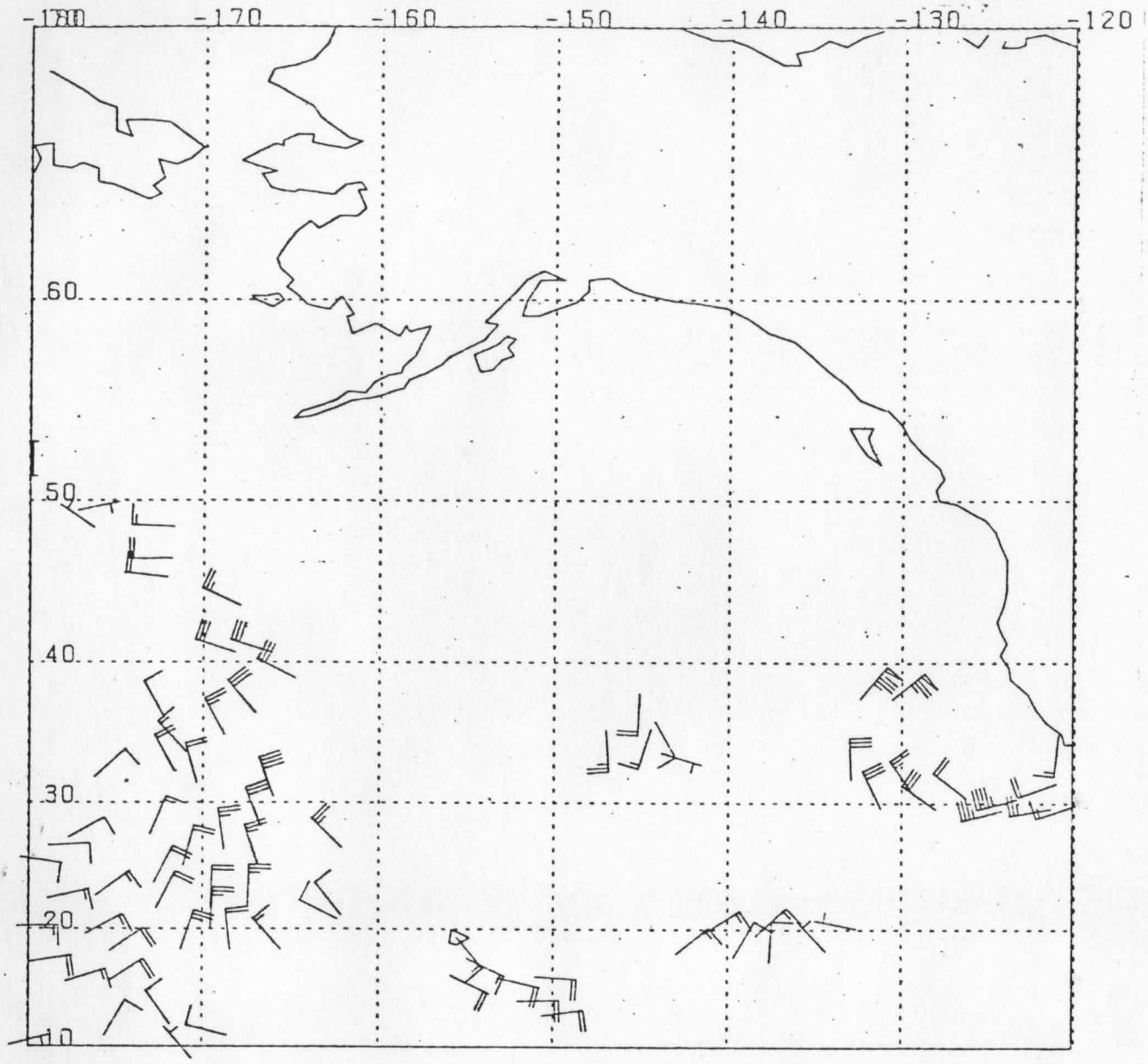

Fig. 8. Mid-level SSEC winds for 7 February 1976

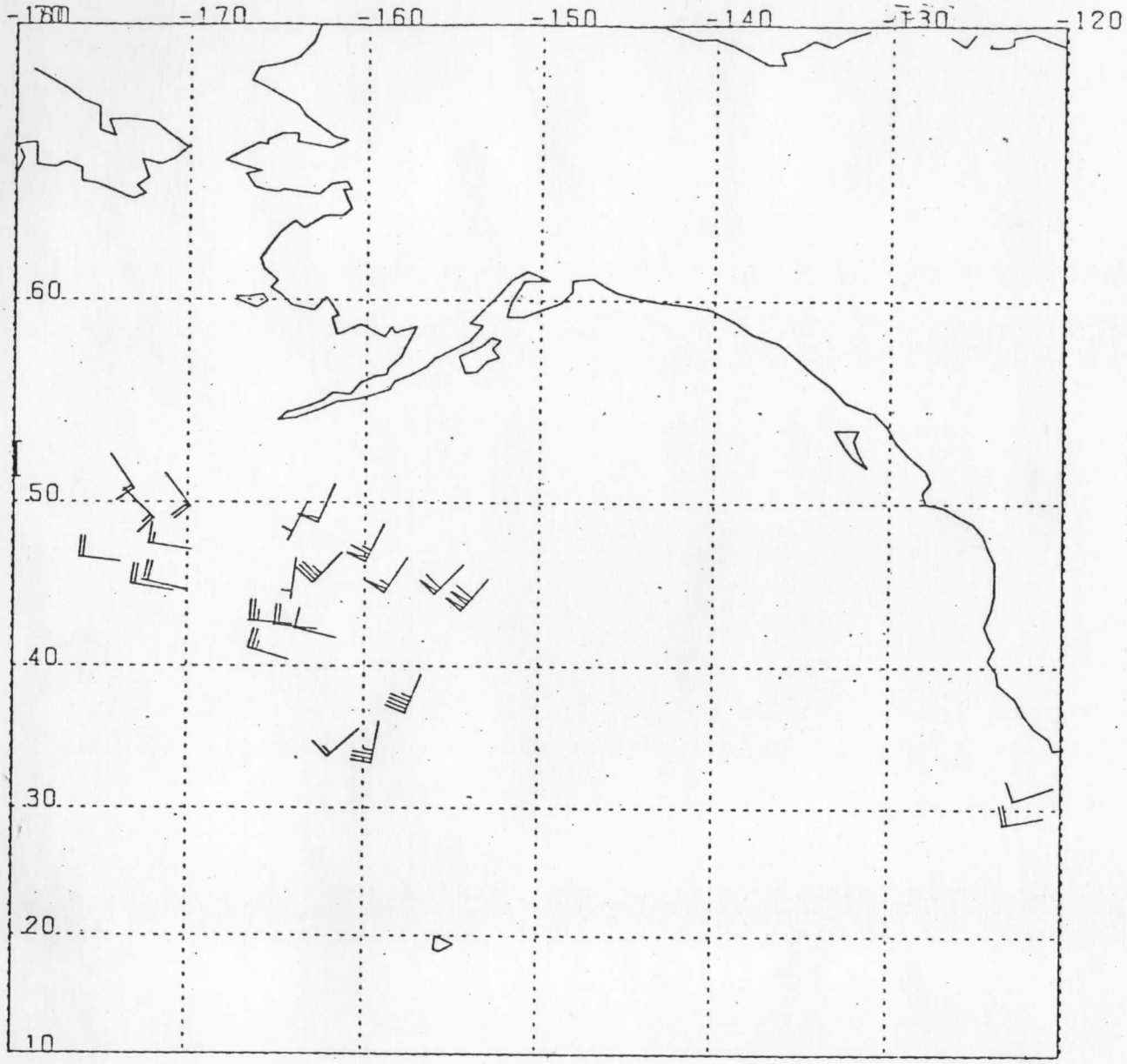

Fig. 9. Mid-level NESS winds for 7 February 1976

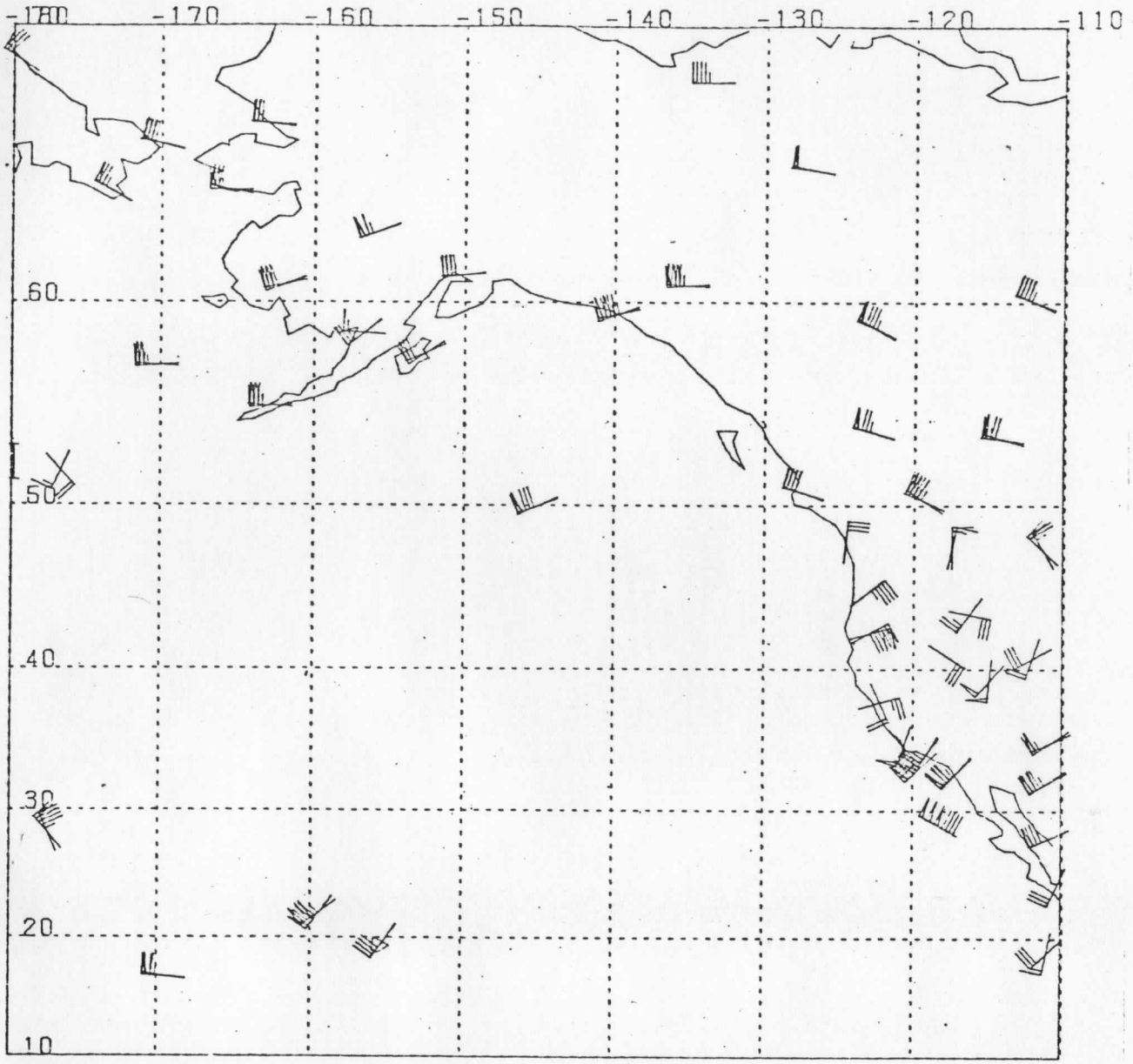

Fig. 10. Mid-level Radiosonde winds for 7 February 1976

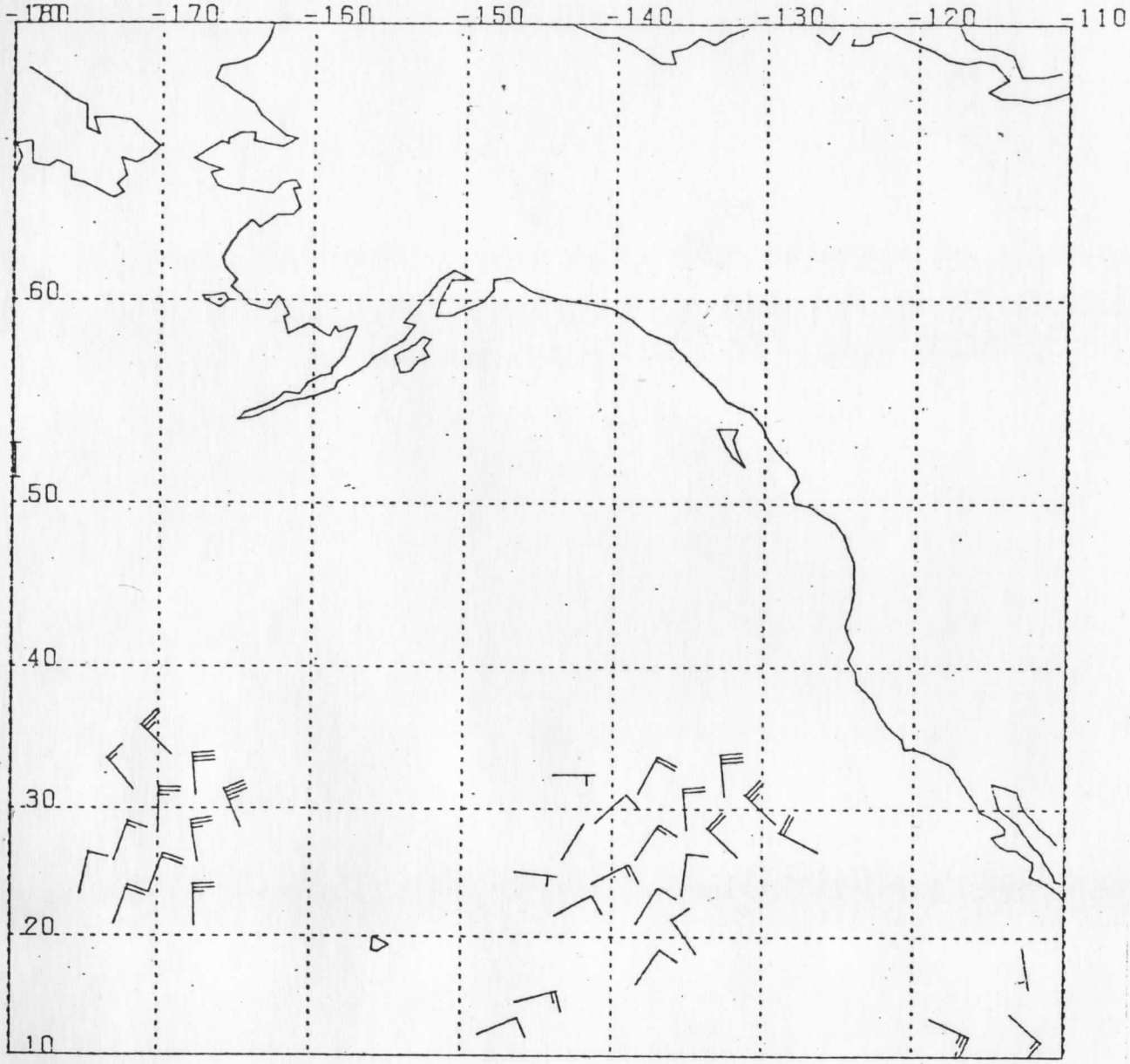

Fig. 11. Low level SSEC winds for 7 February 1976

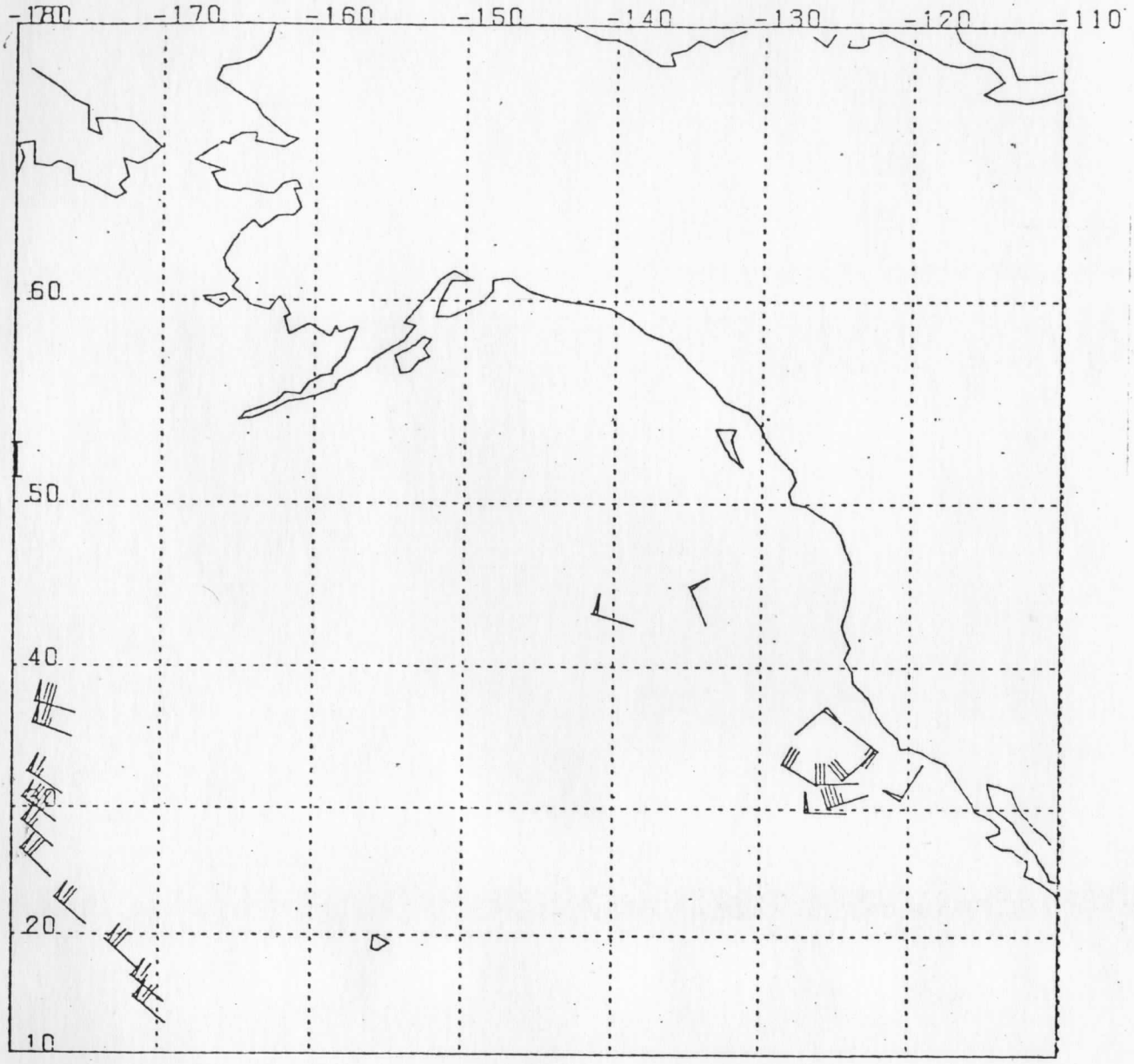

Fig. 12. Low level NESS winds for 7 February 1976

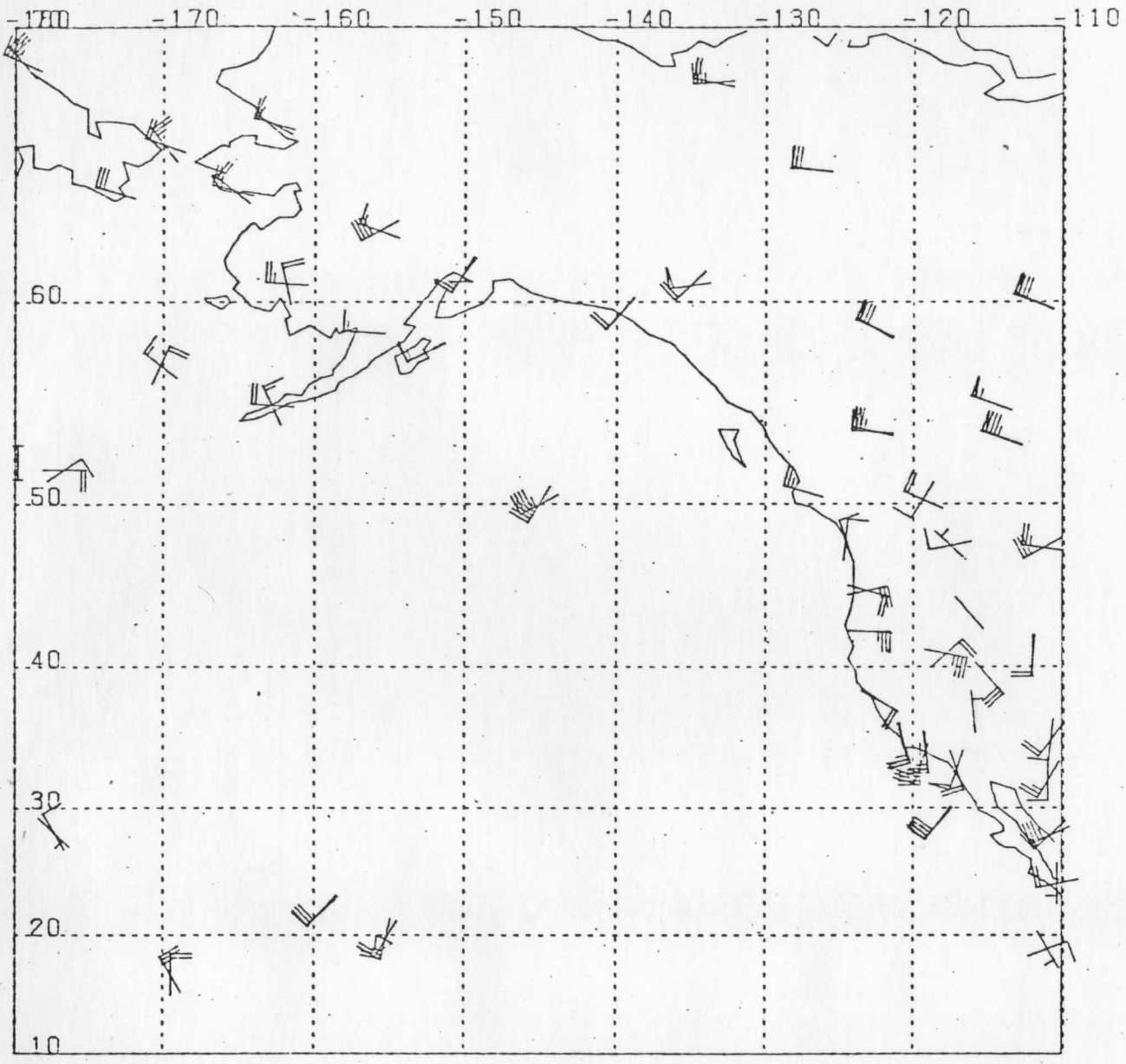

Fig. 13. Low level Radiosonde winds for 7 February 1976

of the target area, and the satellite observation at this level were relatively few and ambiguous. NESS and SSEC satellite derived wind vectors at middle levels suffer from height assignment complications and, therefore, may not provide a good data source by themselves.

The upper level NMC Level III analysis displayed a very large high pressure system over the eastern Pacific (N. Hemisphere). The ridge was very sharp and well defined. The axis of the ridge was oriented from south-southwest to north-northeast. The anticyclone influenced the flow pattern from Hawaii to the Gulf of Alaska. To the southeast along the Baja California coast, a closed low pressure system was positioned ahead of the ridge. This closed low, in front of the ridge, enhanced the steepness of the ridge.

The streamline analysis performed by the McIDAS system at the Space Science Center used a combined data set consisting of NESS and SSEC satellite winds, radiosonde observations and commercial airline reports.

The combined data set provided an excellent streamline depiction of the synoptic flow pattern as reported by NMC (fig. 14). The well defined anticyclonic flow, characteristic of a high pressure system, was placed in the central eastern Pacific exactly where the NMC analysis placed the high. The low off the Southern California coast was also positioned in accordance with the NMC analysis. In the northwestern corner of the target area over the Aleutian Islands a short wave cyclone was present. In the course of this event the short wave moved rapidly across Alaska and became a significant feature along the North American coast.

The isotach minimum was located on the west side of the anticyclone near the crest of the ridge (fig. 15). The jet core exceeded 60 m s^{-1} and was oriented along a SW-NE line. On the near side of the ridge another

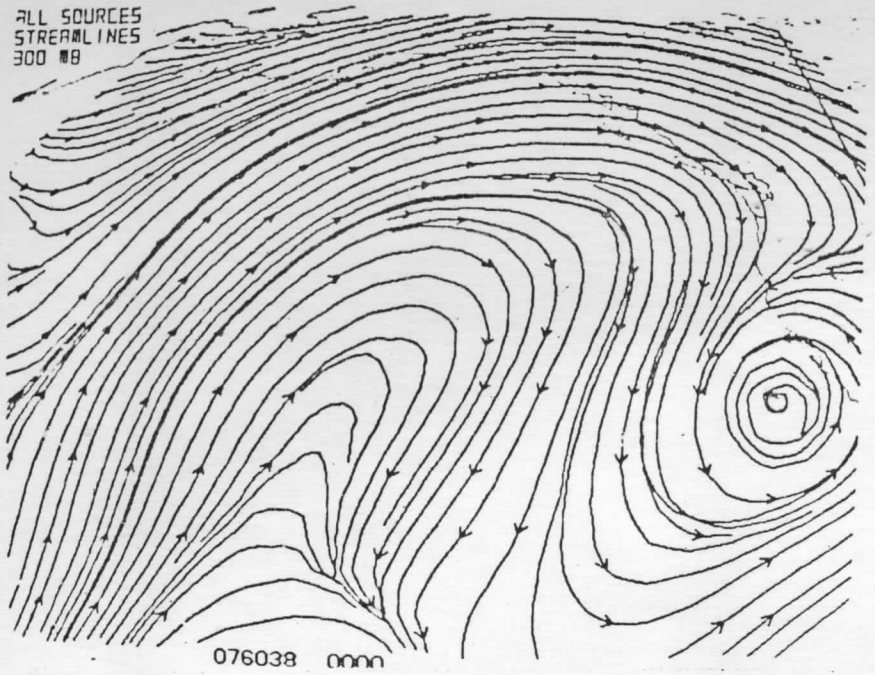

Fig. 14. Streamline analysis of the combined upper level wind set for 7 February 1976

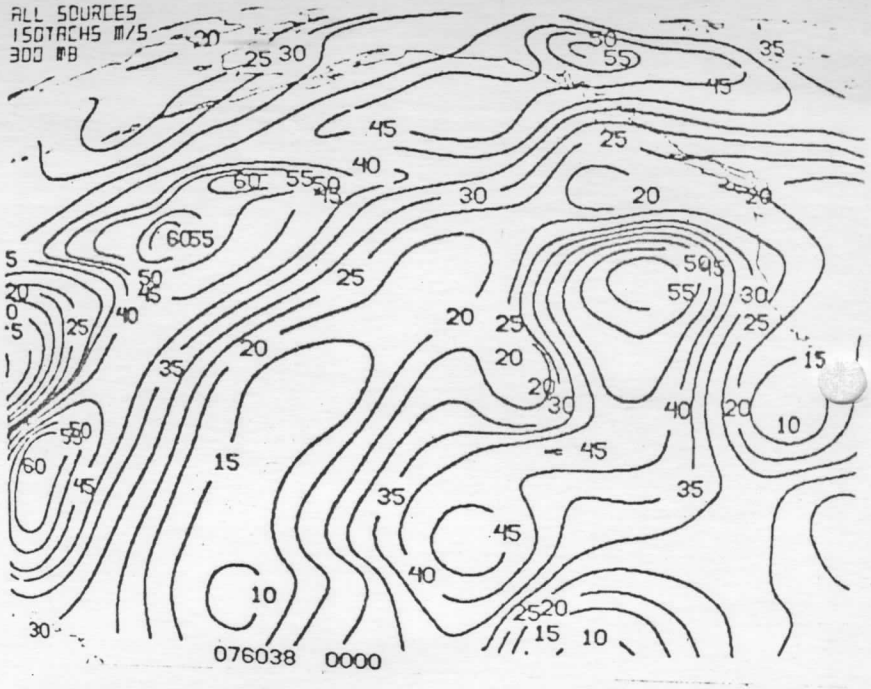

Fig. 15. Isotach analysis of the combined upper level wind set for 7 February 1976

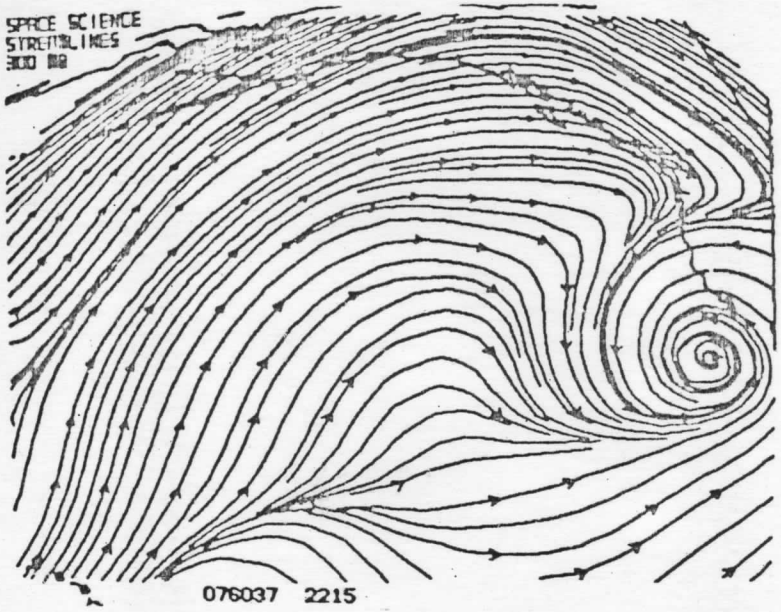

Fig. 16. Streamline analysis of the SSEC upper level wind set for 7 February 1976

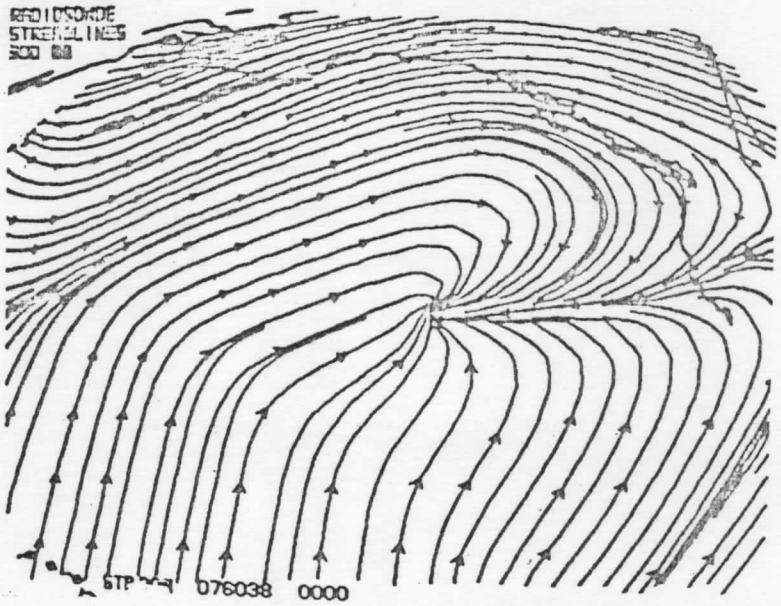

Fig. 17. Streamline analysis of the radiosonde upper level wind set for 7 February 1976

isotach maxima was centered with a top wind speed of 55 m s^{-1}. The polar jet wrapped itself around the ridge with a break about the crest of the ridge.

Separate streamline and isotach analyses of the individual data sets revealed the nature in which the winds were gathered. Over the ridge the clouds were few and ill defined. The SSEC streamline analysis placed a ridge in the Pacific, but with a reduced amplitude (fig. 16). The Southern California low on the other hand was extremely well defined with a tight circular cyclonic flow pattern. This result was expected since the satellite winds require many clouds for "wind getting." The flow pattern around the low was described quite nicely by the cloud drift vectors. Radiosondes could not handle the large anticyclone in the Pacific (fig. 17). The lack of observations in this region resulted in a poor analysis. The NESS analysis also relied on satellite methods for obtaining wind vectors, but because of far fewer vectors (79 NESS vs 543 SSEC) the NESS streamline analysis was on the whole unreliable (fig. 18). Finally the aircraft observations produced a streamline analysis which outlined the well defined ridge (fig. 19). The aircraft reports provided an excellent upper level wind set. Only over Alaska did the streamline field go awry due to a lack of observations in the northern latitudes.

The individual wind speed fields produced varied isotach analyses. There were plausible analyses by both SSEC and the aircraft data sets, and weaker analysis by the NESS and radiosonde sources (figs. 20-23). The SSEC and aircraft sets complimented each other. Both sets filled in gaps in the wind field and ultimately produced a better combined analysis. Further analysis of the succeeding days reveals the strengths and weaknesses of the many data sources.

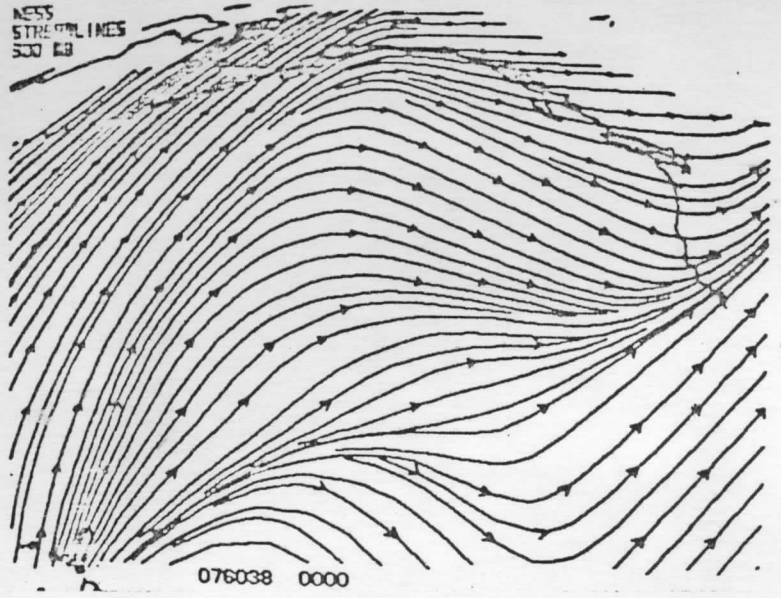

Fig. 18. Streamline analysis of the NESS upper level wind set for 7 February 1976

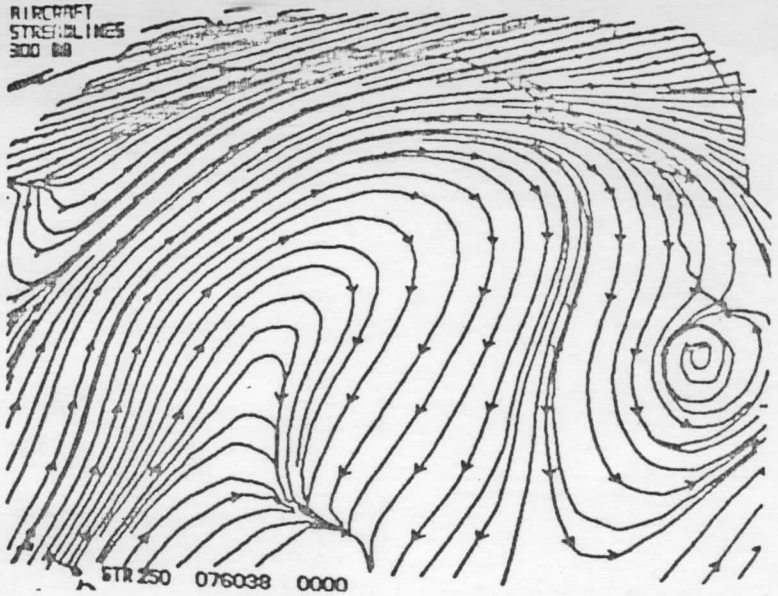

Fig. 19. Streamline analysis of the aircraft upper level wind set for 7 February 1976

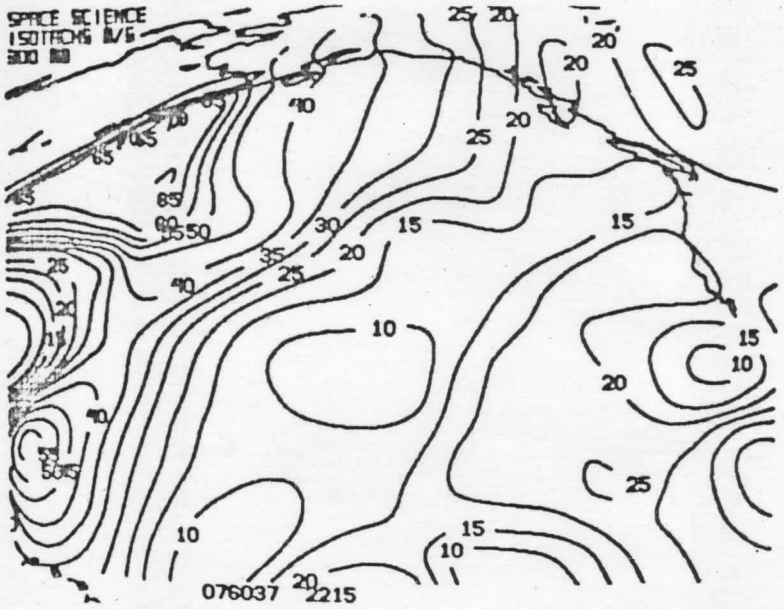

Fig. 20. Isotach analysis of the SSEC upper level wind set for 7 February 1976

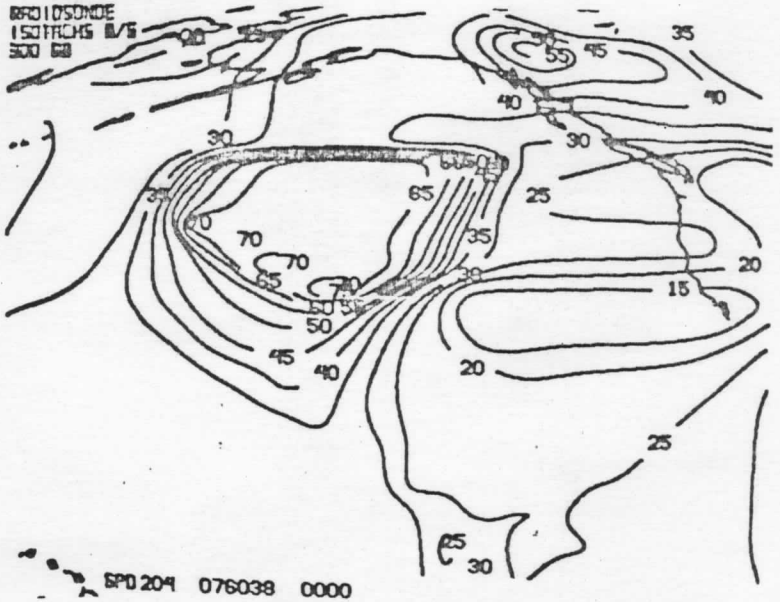

Fig. 21. Isotach analysis of the radiosonde upper level wind set for 7 February 1976

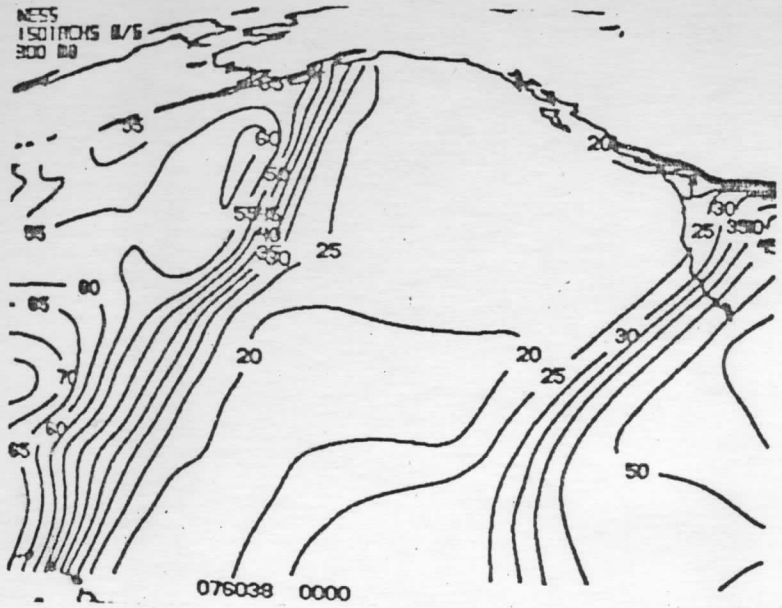

Fig. 22. Isotach analysis of the NESS upper level wind set for 7 February 1976

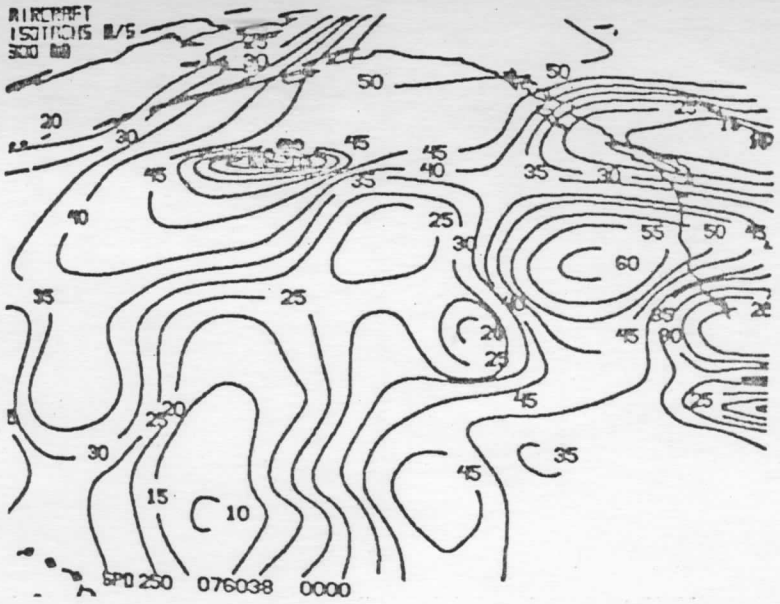

Fig. 23. Isotach analysis of the aircraft upper level wind set for 7 February 1976

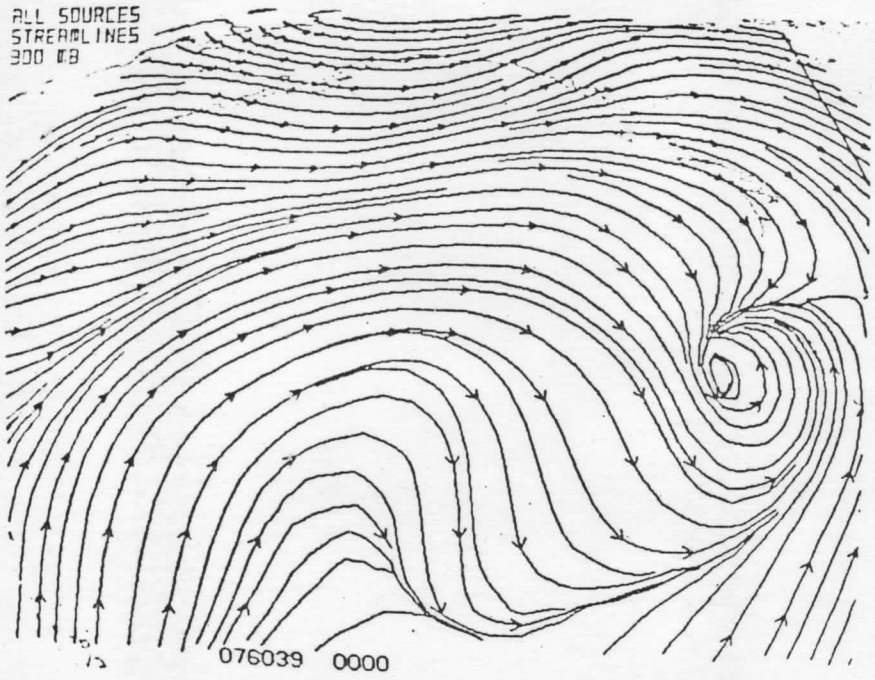

Fig. 24. Streamline analysis of the combined upper level wind set for 8 February 1976

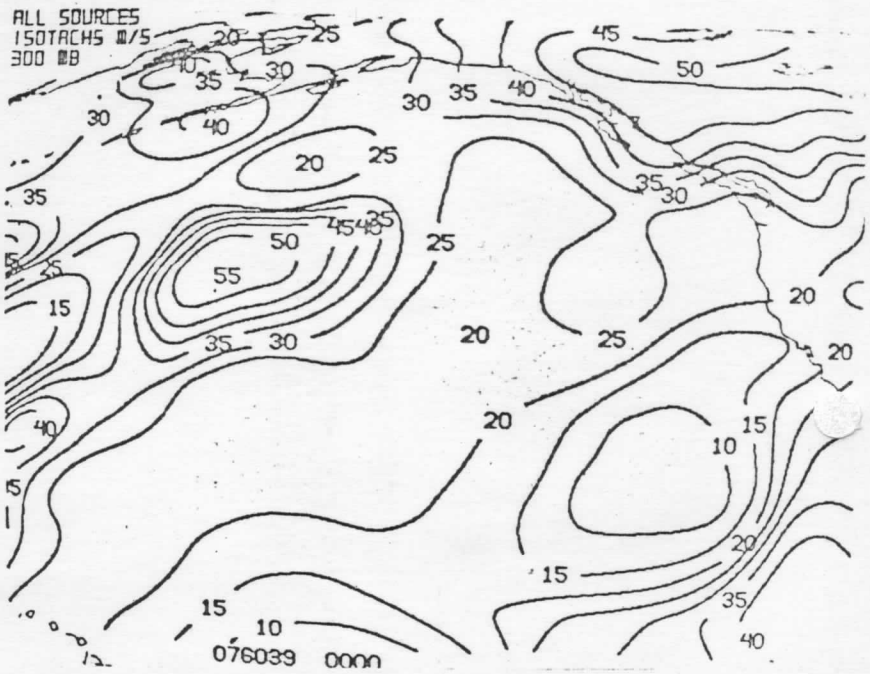

Fig. 25. Streamline analysis of the combined upper level wind set for 8 February 1976

The 300 mb NMC Level III analysis for the eastern Pacific on day 39 at 0000 GMT continued to show a large high pressure system dominating the center of the target area. The height contours indicated the amplitude of high pressure wave was roughly 30° latitude with the center of the ridge now located at 35°N and 140°W. Immediately to the east along the Southern California coast lay a small low pressure system. The axis of this closed low ran from the SW to the NE. To the north along the Alaskan coast was a short wave trough. The polar jet was located on the back side of the crest of the ridge, along the convergence zone between the Pacific high pressure ridge and the Aleutian short wave trough. A central core speed in excess of 45 m s^{-1} was recorded south of Anchorage over the Gulf of Alaska. The jet core was oriented along a SW-NE axis.

The upper air streamline analysis performed at the Space Science Center contained essentially the same analysis. The combined data set produced by SSEC, NESS, and radiosonde wind sets (fig. 24) placed the mid-Pacific ridge in the same location as the NMC analysis. The aircraft observations were insufficient for this time period and could not produce an adequate analysis. The low along the Southern California coast also appeared and was oriented along a SW-NE line. However, it was centered slightly to the east of the NMC analysis. The radiosonde data recorded the movement of the short wave Aleutian low as it migrated eastward over Alaska. Neither the NESS nor SSEC observations accurately noted this movement. The combined data set was dependent upon radiosonde reports in the northern latitudes. Conversely the combined data set was dependent upon the satellite over the Pacific Ocean. The radiosonde observations failed to record a slight weakening of the high pressure ridge over the 24 hr period from 0000 GMT on day 38 to 0000 GMT on day 39.

A similar result was apparent with the isotach analysis (fig. 25). The radiosondes filled in the isotach field over Alaska, whereas the isotach field over the Pacific Ocean was described by satellite (SSEC and NESS) observations. Without the latter sources the strength and position of the jet core could not be represented accurately. The combined analysis positioned the jet core along the convergence zone between the mid-ocean ridge and the Aleutian low.

The 850 mb NMC analysis for 0000 GMT on day 39 was dominated by the Aleutian low and not by the Pacific high. A tightly packed height gradient existed along the axis of the low as it extended southward along the 140th meridian. The cyclone was centered at 60°N and 140°W. This placed the center of the low along the Alaskan coastline near the Alaskan-Yukon border line. The trough moved rapidly eastward from its previous position. Off the Southern California coast the closed cyclone was present. The presence of these two cyclones limited the influence of the anticyclone on the North American coast. A col point off the Oregon coast existed between the two cyclones and the anticyclone.

The analysis performed by the McIDAS software confirmed the major synoptic features mentioned in the NMC analysis. The differences that occurred were a result of comparing streamlines to a height contour field. Certainly a frictionless approximation cannot be made at this low level but, nevertheless, a comparison of the streamline and height contours analysis was informative. The advantage of the combined data set over the NMC analysis was an insight into streamline and isotach patterns in the western Pacific. The NMC analysis could not reveal smaller scale streamline perturbations and isotach variability. The McIDAS analysis was able to identify isotach minima and maxima not available in the NMC analysis. This

information was obtained by the broad satellite data coverage and not by radiosondes which are restricted in number and location (fig. 26-29).

By 0000 GMT on day 40 a significant change in the upper level atmospheric structure had occurred. The NMC 300 mb analysis showed a combining of the two low pressure systems. As the short wave trough over Anchorage moved east it merged with the Southern California low to form a large longwave trough centered off the central California coast. The Pacific high pressure ridge weakened and migrated westward to the edge of the target area. The result was a deep trough extending from the Gulf of Alaska down to Baja California.

The isotach pattern revealed a maximum at the top of the ridge, near the Aleutian Islands, and a relative minimum at the base of the trough. The maximum wind speeds reached were 60 m s^{-1}, while the minimum speed along the trough only attained 10 m s^{-1}.

The McIDAS analysis of the combined data set produced a streamline analysis which reflected the merging of the two low pressure systems (fig. 30-31). The streamline analysis for day 40 depicted a large anticyclonic flow pattern covering most of the target area. The trough dug in along the eastern border and a cyclonic flow pattern was quite evident along the North American coast.

The individual data sources were varied in their upper level streamline analyses. Since the long wave trough was located along the coast the radiosonde reports picked up its position. These same stations, however, could not adequately describe the position and structure of the anticyclone. The satellites and aircraft reports did a very good job in defining the clockwise flow of the anticyclone over the Pacific. The aircraft reports could not properly analyze the flow pattern in the northern latitudes due

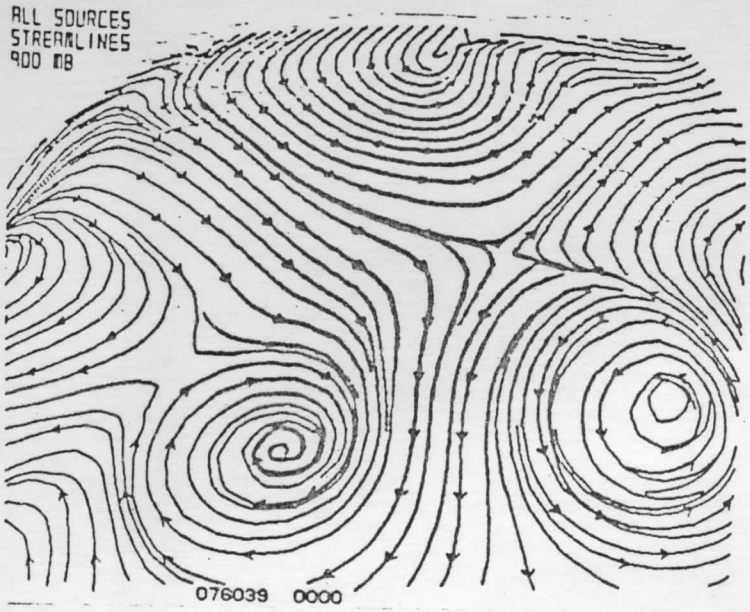

Fig. 26. Streamline analysis of the combined lower level wind set for 8 February 1976

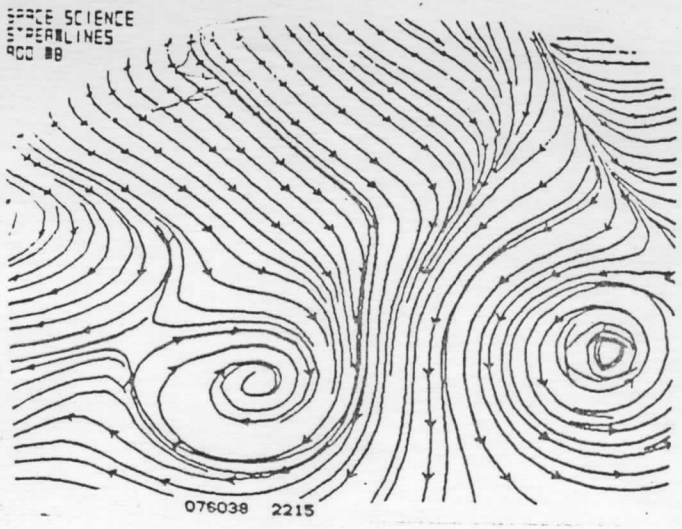

Fig. 27. Streamline analysis of the SSEC lower level wind set for 8 February 1976

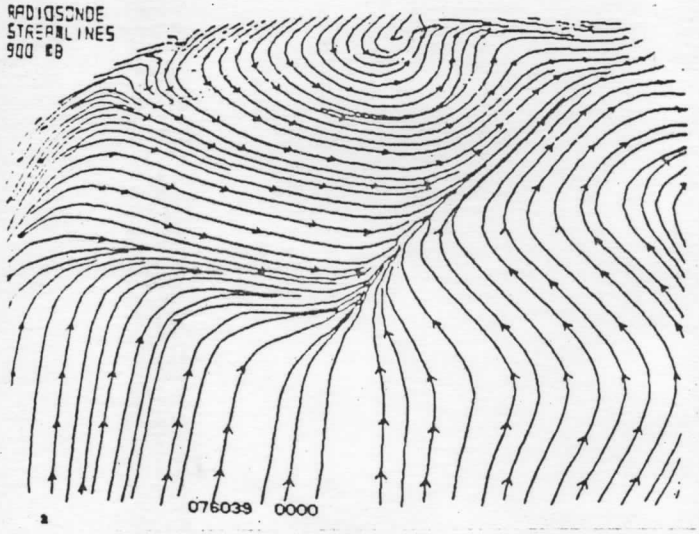

Fig. 28. Streamline analysis of the radiosonde lower level wind set for 8 February 1976

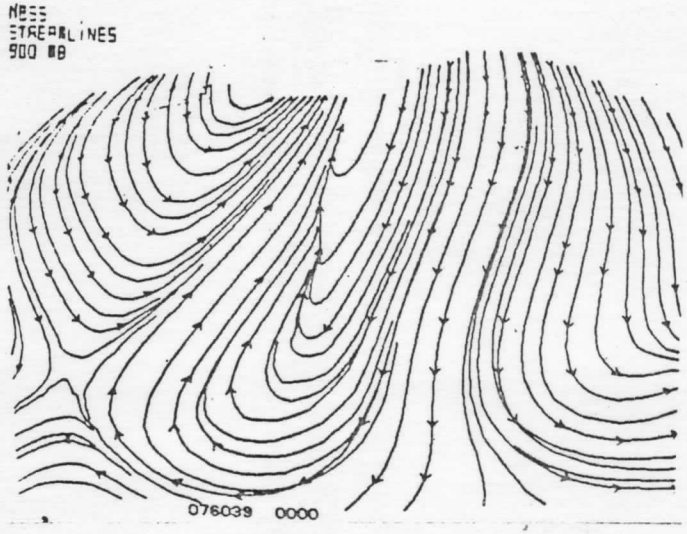

Fig. 29. Streamline analysis of the NESS lower level wind set for 8 February 1976

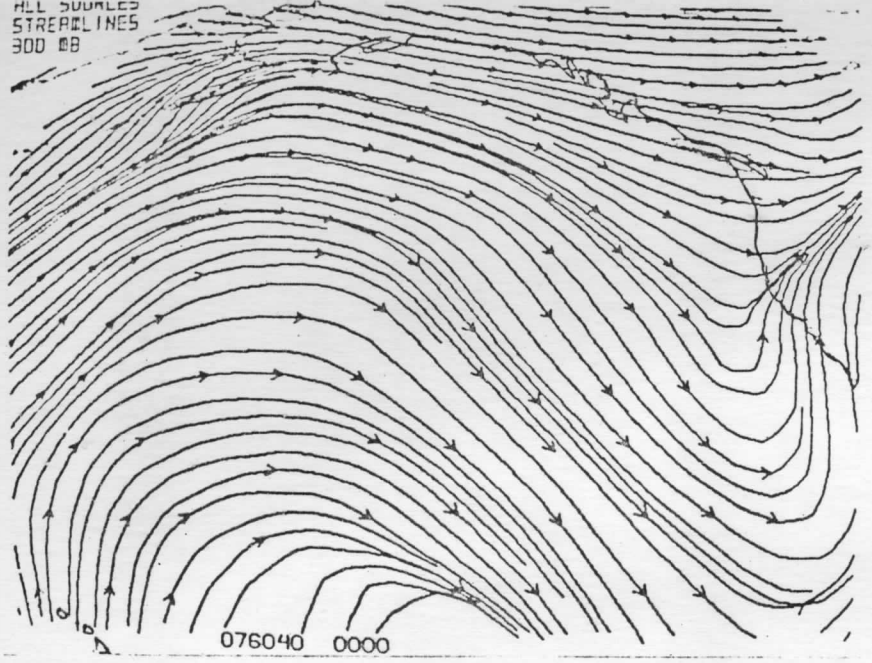

Fig. 30. Streamline analysis of the combined upper level wind set for 9 February 1976

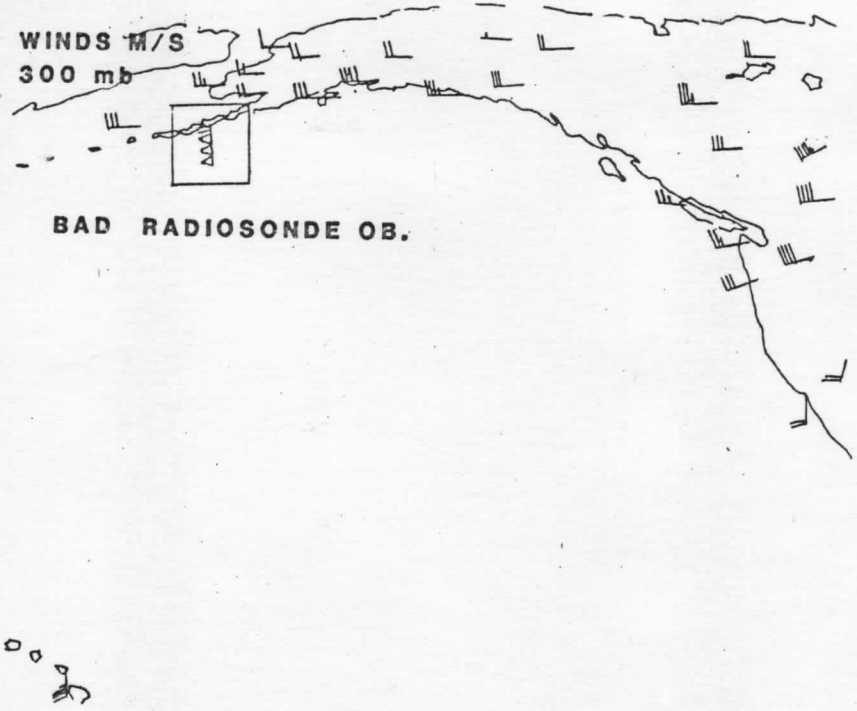

Fig. 32. Erroneous radiosonde upper level wind observation for 9 February 1976

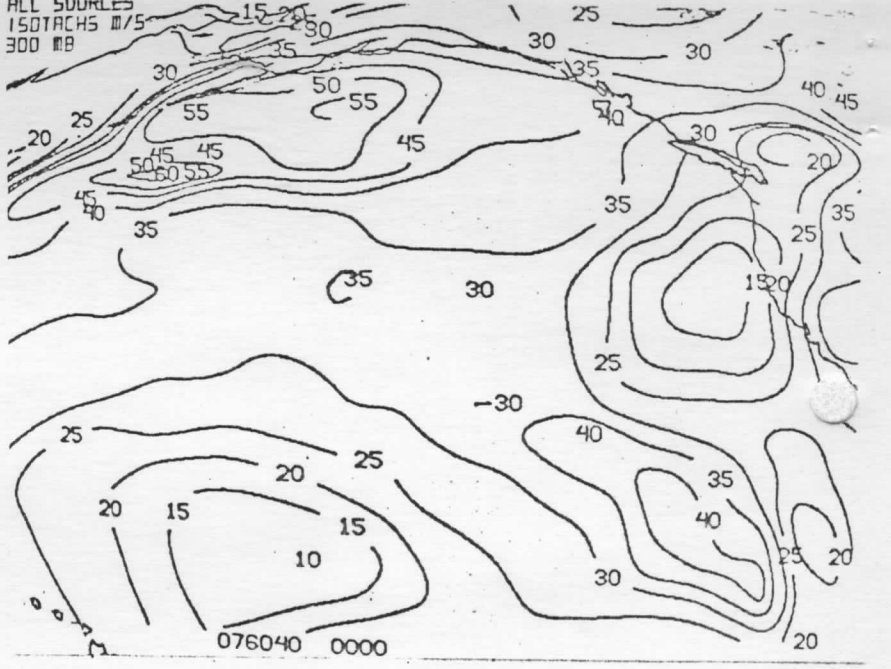

Fig. 31. Isotach analysis of the combined upper level wind set for 9 February 1976

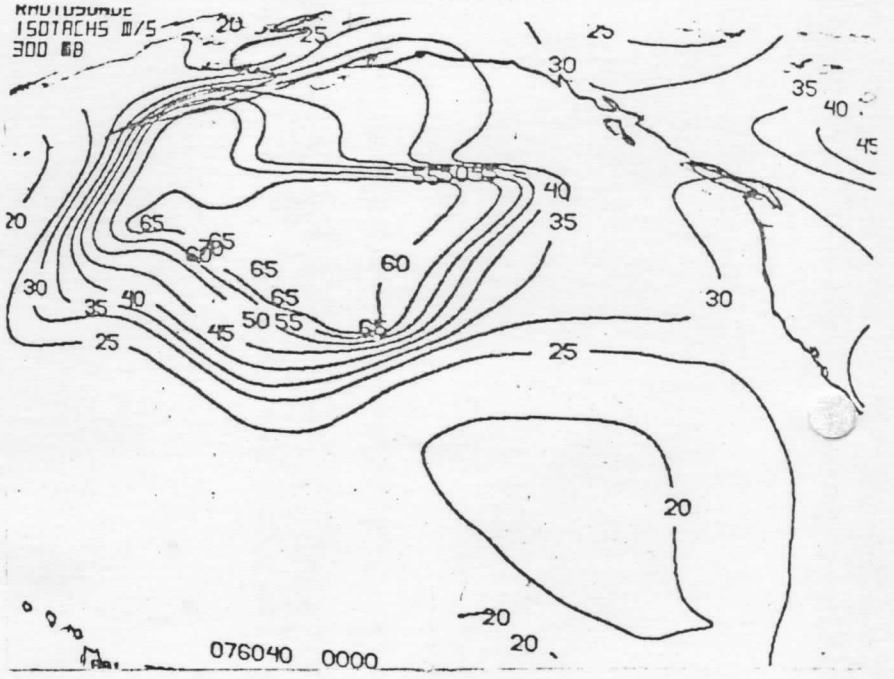

Fig. 33. Isotach analysis of the corrected radiosonde upper level wind observation for 9 February 1976

to a lack of observations in that region. However, the aircraft reports over the middle of the target area did produce a reasonable streamline and isotach analysis.

The individual isotach patterns were also varied in their analysis. Neither NESS nor SSEC could properly locate the jet maximum. Both of the sources produced an analysis with broad region of 35-40 m s^{-1} without a sharply defined center. Aircraft reports, on the other hand, pinpointed the well defined jet cores with 55-60 m s^{-1} winds. The radiosonde report for 0000 GMT on day 40 illustrated the effect of a single bad observation on the isotach field. Figure 32 outlines the bad observation (170 m s^{-1}) and locates its position over the Aleutian Islands. The resulting isotach analysis was distorted and erroneous. When the bad observation was removed from the data set a more plausible isotach analysis was produced (fig. 33). Although, the radiosonde isotach analysis over the ocean was still localized and point specific.

A combination of all four data sources (SSEC, NESS, aircraft and a corrected RAOB data set) produced a very good isotach pattern over the entire target area. The radiosonde reports filled in the northern region of the target area, while the NESS and SSEC reports supplemented the aircraft observations.

At lower levels (850 mb NMC analysis) the short wave associated with the Gulf of Alaska storm began to move eastward. The axis of the storm rotated from a north-south orientation to an east-west one. As a result the flow became somewhat zonal in nature. Unlike the upper level pattern the Southern California cyclone remained distinct from the Aleutian low and remained anchored off the coast.

The low level McIDAS analysis relied primarily on the radiosonde data

to the north and SSEC satellite winds over the water. NESS observations were few but did compliment the SSEC satellite winds. The NESS winds were helpful in locating the Southern California storm system. The streamline analysis performed on the SSEC data produced a double centered anticyclone in the left center of the target area. None of the other sources could verify the existence of the double center and, therefore, it was ignored in the combined data set analysis. The radiosonde analysis provided the observations to locate the low pressure system over Alaska. Although the radiosonde data was completely lacking in the mid-Pacific it was the sole source to identify the Alaskan low.

The final day analyzed in the first case was February 10th (day 41). The 300 mb NMC analysis showed the intensification of the long wave trough. The axis of the trough was now oriented along a SW-NE line. In addition, the Pacific high began to strengthen and rebuild in the central eastern Pacific. The ridge now stretched from Hawaii to Alaska. The low which was located in the Gulf of Alaska migrated eastward over British Columbia and merged with the Southern California cyclone to form the large, full latitude trough.

The McIDAS combined data set analysis also displayed the intensification and eastward migration of the long wave trough. The target area was completely dominated by the clockwise flow of the high pressure ridge. Only on the eastern boundary of the target area does a glimpse of the trough show up. The radiosonde, satellite and aircraft analyses are all similar. All four data sources indicate the presence of the mid-ocean anticyclone. The reason for the similarity in all the data sets was the lack of a cyclone in the northern latitudes. The satellite and aircraft analyses extrapolate

data from the center of the target area into the northern latitudes. Since the ridge dominated a major portion of the target area the extrapolation resulted in a reasonable analysis in the northern latitudes. Likewise, the radiosonde analysis relied on Ocean Station Papa and Hawaii for its mid-ocean data. In this particular synoptic case those two stations provided sufficient information to allow a reasonable extrapolation of the data.

The isotach analysis displayed a long jet core along the crest of the ridge with maximum wind speeds of 55 m s^{-1}. A speed minimum was again located at the base of the trough. The jet core progressively moved eastward as the Aleutian cyclone migrated over Canada and merged with the Southern California low.

The lower level analysis was also dominated by the semi-permanent high pressure system. The anticyclonic synoptic flow pattern was centered in the target area. The streamline analysis detected a cyclonic wind flow in the northwest corner of the target area. This was the first indication of a new storm approaching form the west. Satellite imagery picked up a cloud mass with no appreciable organization. Due to the curvature of the earth, reliable cloud drift winds could not be produced. The radiosonde reports on the other hand were able to establish the cyclonic flow pattern and were responsible for the analysis of this new cyclone.

4. Case II: February 14-16, 1976

The second synoptic event covered the time period from February 14-16, 1976 (Julian days 45-47). The synoptic weather pattern was completely different from the first event. Instead of an anticyclone dominating the Pacific, a long wave trough was positioned over the target area. The 300 mb atmospheric structure on day 45 consisted of a long wave trough along the eastern half of the target. The axis of the trough was primarily north to

south along the 130° W meridian. To the west the flow was predominantly zonal through the northern latitudes. Near Hawaii the flow was northerly as a result of a high pressure ridge which was located to the southwest of Hawaii. The ridge extended north to the center of the target but was not particularly strong.

The NMC isotach pattern showed a strong jet near the western boundary. Maximum wind speeds were 55 m s^{-1} at 48°N and 170°W. Another jet core was located on the cyclonic shear side of the long wave trough. The flow was to the northeast at 45 m s^{-1}. An isotach minimum separated the two jet cores along the base of the trough.

The streamline analysis performed by McIDAS on the combined satellite, radiosonde, aircraft observations differs from the NMC analysis in the positioning of the axis of the Pacific trough (fig. 34). The combined data set analysis consisted of a trough anchored along the Washington coastline. Its axis was oriented north to south. A second short wave trough was located to the southwest with a southwest to northeast axis. This analysis differed from the NMC analysis, which maintained the presence of one full latitude trough and not two short wave troughs out of phase with each other.

The satellite and aircraft observations were responsible for pinpointing the presence of the shortwave east of Hawaii. The SSEC streamlines were not as amplified as the aircraft analysis. The NESS streamlines were the only analysis which did not depict a cyclone in the northern latitudes along the American-Canadian coastline. The NESS analysis simply lacked the necessary vectors in this region and, therefore, failed to locate the coastal cyclone.

The combined isotach analysis (fig. 35) picked up a very strong jet upstream from the northern trough. Core speeds of 80 m s^{-1} along the tip

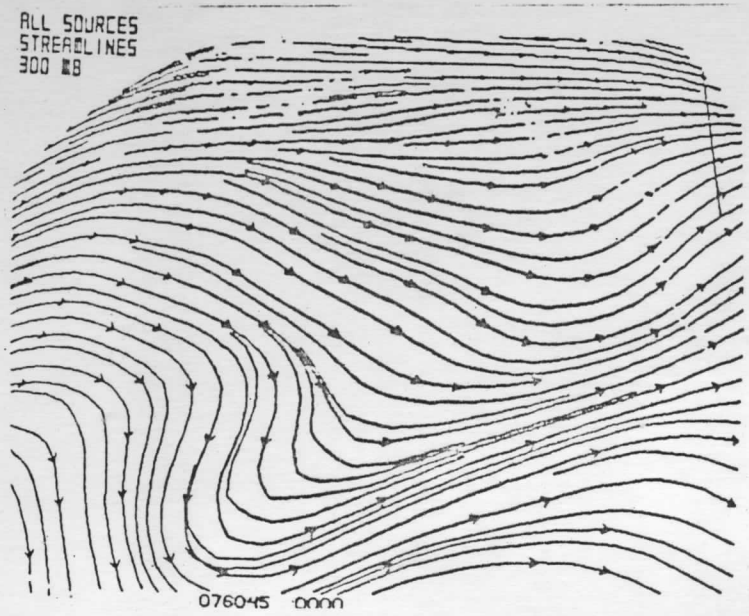

Fig. 34. Streamline anlaysis of the combined upper level wind set for 14 February 1976

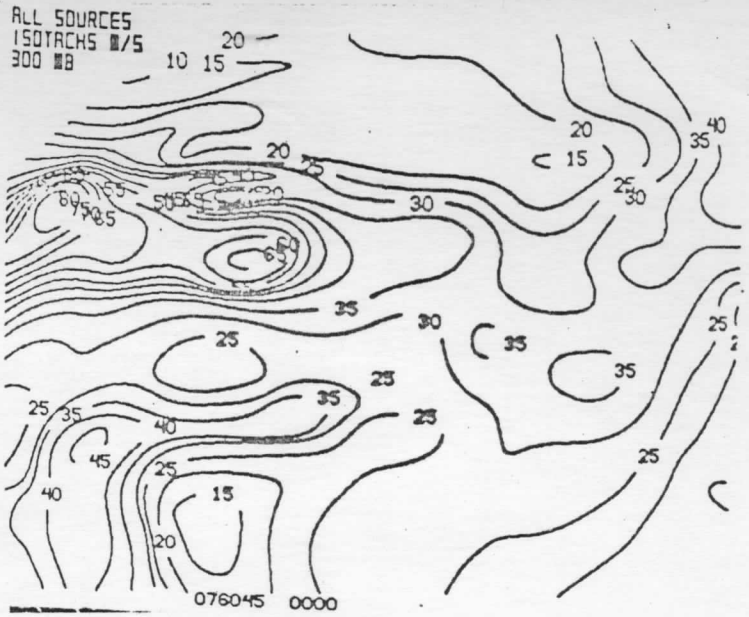

Fig. 35. Isotach analysis of the combined upper level wind set for 14 February 1976

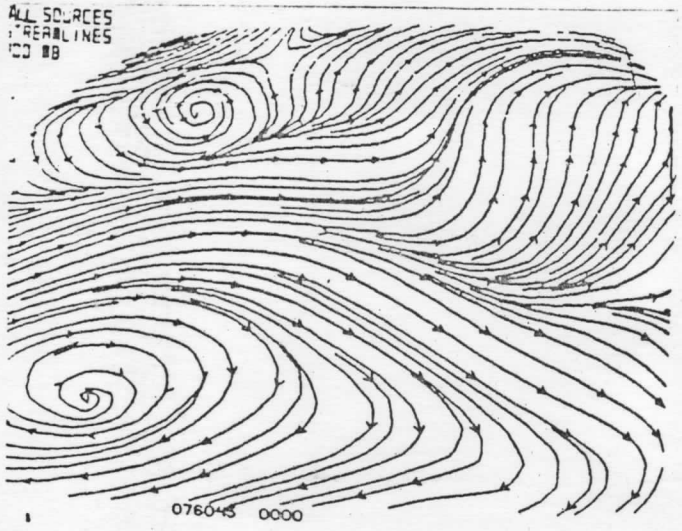

Fig. 36. Streamline analysis of the combined lower level wind set for 14 February 1976

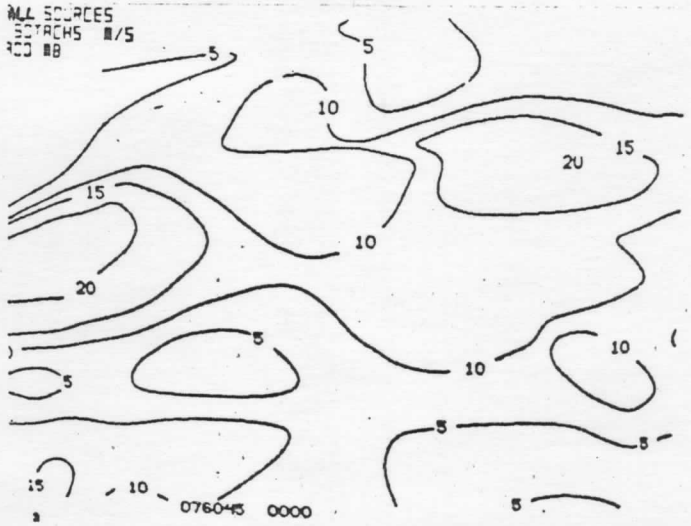

Fig. 37. Isotach analysis of the combined lower level wind set for 14 February 1976

of the Aleutian Islands were recorded. Another center was located east of the Aleutians in the Gulf of Alaska. This isotach analysis provided a more detailed analysis than the NMC analysis. Minimum 300 mb wind speeds (10-15 m s^{-1}) were noted along the base of both troughs. Only the aircraft and SSEC observations did an adequate job on the wind speed analysis. The other sources failed beacuse of a lack of observations. When these reports were incorporated into a combined data set they provided valuable information towards the production of a complete analysis.

The lower level (850 mb) NMC analysis indicated the presence of a low pressure system over the Aleutian Islands, and a trough further east in the Gulf (figs. 36-37). A broad high pressure system dominated the lower latitudes. It was centered just north of the Hawaiian Islands and stretched as far east as the California coast. The streamlines produced on McIDAS were via the radiosonde and SSEC reports. The NESS observations were too few to present a valid individual analysis. The radiosonde reports in the northern latitudes enabled the streamlines to pick up the cyclone located over the Aleutian Islands. The SSEC analysis could not adequately obtain cloud motion vectors for this region due to limb effects. On the other hand the satellite wind vectors were the only reports which could verify the anticyclonic flow in the middle of the Pacific. The radiosonde reports from Ocean Station Papa and Hawaii were not sufficient to describe the total synoptic flow pattern. Together the two sources worked together to produce a streamline analysis for the low level wind field.

By 0000 GMT on February 15, 1976 (Julian day 46) the long wave trough depicited by the NMC analysis moved eastward and was now centered over the west coast of the continental United States. The trough axis was still oriented from the north to the south. The Hawaiian high built in from

the west and the associated anticyclonic flow was felt across the entire eastern Pacific.

The combined data set was almost entirely dependent upon satellite wind observations (fig. 38). The aircraft reports did not fall within the bounds of the target area. Consequently, the analysis relied on the SSEC and NESS satellite winds, and the radiosonde observations. The radiosonde reports, as mentioned before, were essentially restricted to North America and, therefore, the entire portion of the target area over the ocean was only subject to satellite cloud drift observations. There were 213 NESS observations and 457 SSEC observations. The satellite winds did an excellent job in depicting the streamline flow pattern over the Pacific Ocean. The analysis complimented the NMC height contours. The streamline trough and ridge positions coincided with the locations of the longwave trough and the Pacific ridge depicted by the NMC analysis.

The isotach analysis for day 46 at 0000 GMT (fig. 39) was dependent upon the satellite and radiosonde observations. Like the streamlines the SSEC and NESS observations proved far more valuable than the radiosonde reports. Again this was a result of the major synoptic features being located over open water away from the radiosonde stations. The jet maximum was curved around the crest of the ridge. The crest was centered over the Gulf of Alaska. The only radiosonde station nearby was Ocean Station Papa. If the polar jet was located over a land mass then the radiosonde reports would most likely have done an excellent job. The jet core was over the water and, thus, the radiosonde reports produced an erroneous isotach analysis. The SSEC and NESS isotach field displayed a lengthy jet with speeds in excess of 75 m s^{-1}. This core had migrated eastward from a position at the tip of the Aleutians on day 45 to the center of the Gulf on day 46.

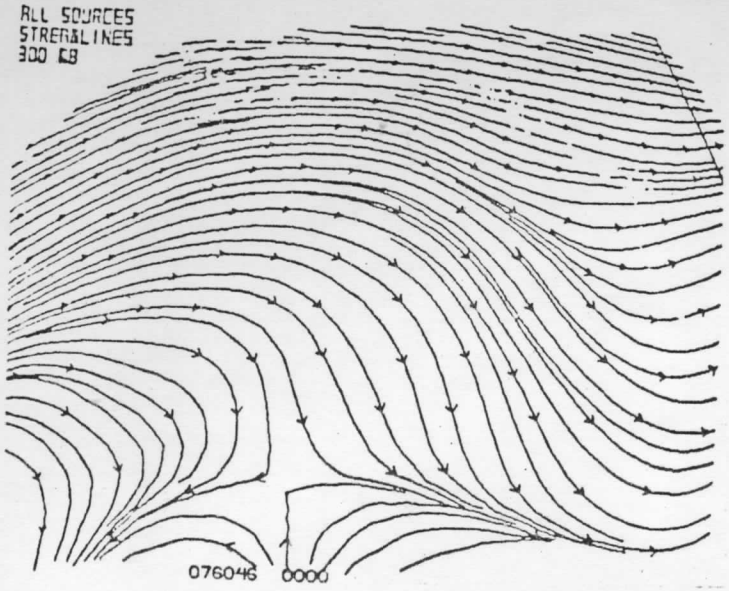

Fig. 38. Streamline analysis of the combined upper level wind set for 15 February 1976

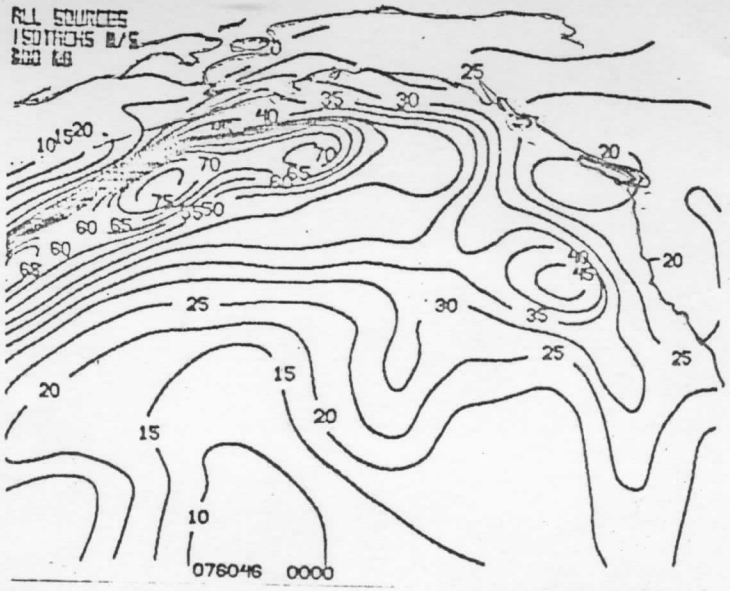

Fig. 39. Isotach analysis of the combined upper level wind set for 15 February 1976

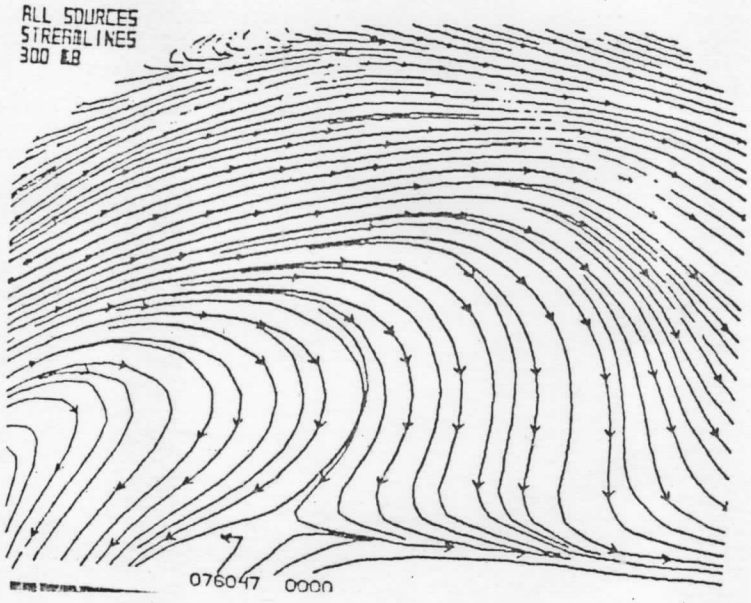

Fig. 40. Streamline analysis of the combined upper level wind set for 16 February 1976

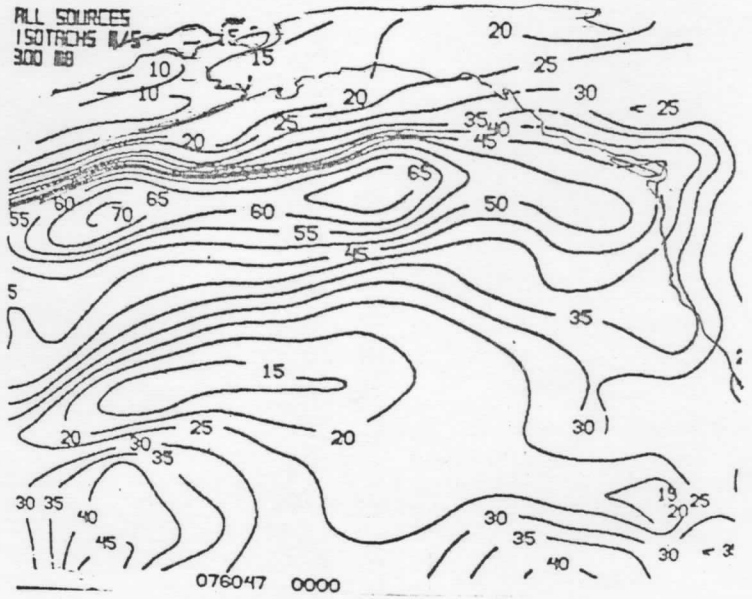

Fig. 41. Isotach analysis of the combined upper level wind set for 16 February 1976

The polar jet was clearly wrapped around the crest of the ridge. Wind speeds dropped off quite rapidly north and south of the jet. The wind speeds over most of the Pacific were roughly 20 m s^{-1} with a minimum less than 10 m s^{-1} just east of Hawaii.

The NMC 850 mb height contours and the combined streamline analysis also complimented each other. Both analyses indicated the eastward migration of the Pacific high and the movement of a new low pressure system into the target area from Siberia. Of course the SSEC streamline analysis failed to detect any cyclonic flow in the northern latitudes, while the radiosonde analysis grossly misrepresented the position and wind flow features of the Pacific anticyclone. Together they provided sufficient information to produce an accurate illustration of the synoptic flow pattern.

On the last day of this event (February 16, 1976) the full latitude trough continued to propagate eastward to a position over the southwestern United States. Behind the trough the 300 mb height pattern was primarily zonal in nature. The anticyclone near Hawaii was not strong enough to move northward and instead it remained in the sub-tropics.

A strong polar jet was associated with a zone of convergence in the north Pacific. A 80 m s^{-1} center was located on the 160°W meridian at 45°N latitude. The jet was elongated along an east-west axis and stretched from the tip of Alaska to the United States coastline.

The McIDAS combined streamline analysis matched the NMC height analysis (fig. 40). A weak anticyclone was evident in the southern portion of the target area and the zonal flow in the north was also apparent. The individual wind sets were generally consistent. Each produced a streamline field with a weak anticyclonic circulation in the southern half of the target area. The SSEC and aircraft analyses had a slightly stronger ridge

but not significantly different from the other streamline analyses.

The isotach analysis produced by the McIDAS software indicated the presence of an elongated jet core stretching from the Aleutians to the west coast of North America (fig. 41). The jet was located north of the Pacific high in a region of strong convergence. There were two centers of maximum wind speed within this jet. The first and strongest maximum (70 m s^{-1}) was positioned just south of the Aleutian Islands. The second maximum (65 m s^{-1}) was over the Gulf of Alaska. The SSEC and aircraft wind sets were most responsible for the isotach field. Both of these sources recorded numerous wind vectors within the polar jet. The radiosonde observation could only supply the Ocean Station Papa data, while the NESS reports were not quite as numerous as the SSEC observations.

The SSEC and aircraft wind sets produced the best analysis for the upper level. The radiosonde and NESS observations were too few to produce a valid analysis on their own. Combined with the SSEC and aircraft data the NESS and radiosonde data integrated nicely to produce the final combined wind field.

5. Case III: February 25-27, 1976

The third event involved in the DST-6 program occurred between February 25-27, 1976 (Julian days 57-58). A brief description of the NMC synoptic analysis follows. A very broad low pressure system was centered in the Gulf of Alaska at the 300 mb level. The base of the trough extended eastward from 160°-125°W longitude. The trough axis was primarily oriented along the 145th meridian. To the west of the broad cyclone was a narrow high pressure ridge which was beginning to amplify. The height contours along the ridge and trough were tightly packed producing a strong polar frontal zone. The jet extended from the backside of the trough around and

through its base. The maximum core wind speed, along the inflection point between the trough and radge, was measured at 65 m s^{-1}. At 20°N latitude and ten degrees longitude east of the Hawaiian Islands a small, poorly organized low pressure system had little effect on the overall synoptic flow in the Pacific.

The McIDAS combined data source analysis did an excellent job in representing the prominent synoptic features at the 300 mb level (fig. 42). The broad low pressure trough was easily identifiable and covered the entire northern half of the target zone. The long broad base of the trough extended from the western to the eastern borders of the analysis. The small weak subtropical low was also evident by the cyclonic nature of the streamline analysis.

An examination of the radiosonde, aircraft and satellite analyses revealed the contribution each source had upon the final analysis. The radiosonde reports over Alaska recorded the presence of the large extra-tropical cyclone. Aircraft reports produced a trough in the Gulf of Alaska but could not center the cyclone. The satellite analyses (NESS and SSEC) could not identify the presence of any cyclonic flow in the northern latitudes, as too few wind vectors were produced in the area above 50°N.

Conversely the satellite reports identified the small cyclone near Hawaii. The cyclone was easily identified from the cloud formation and development. Aircraft flybys around Hawaii also established to presence of the weak trough. Of course the radiosonde observations were insufficient to produce an accurate analysis in the Pacific.

The isotach field for day 56 was best analyzed by the aircraft data. A long jet core along the entire base of the trough was clearly defined by the aircraft observations. The SSEC isotachs produced a similar analysis

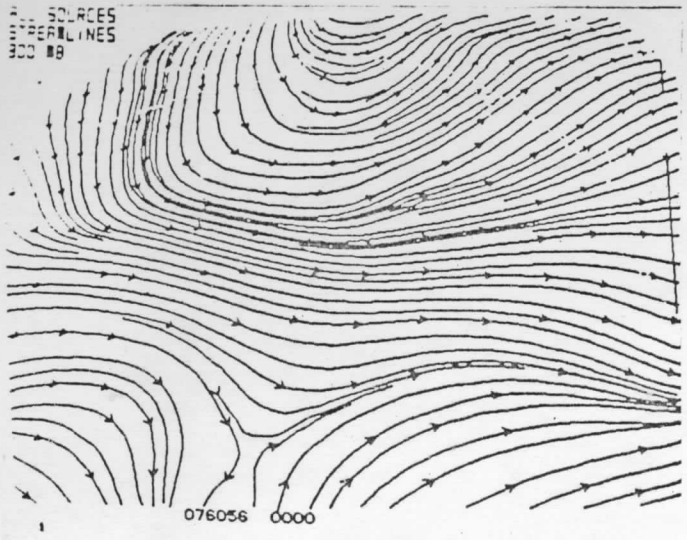

Fig. 42. Streamline analysis of the combined upper level wind set for 25 February 1976

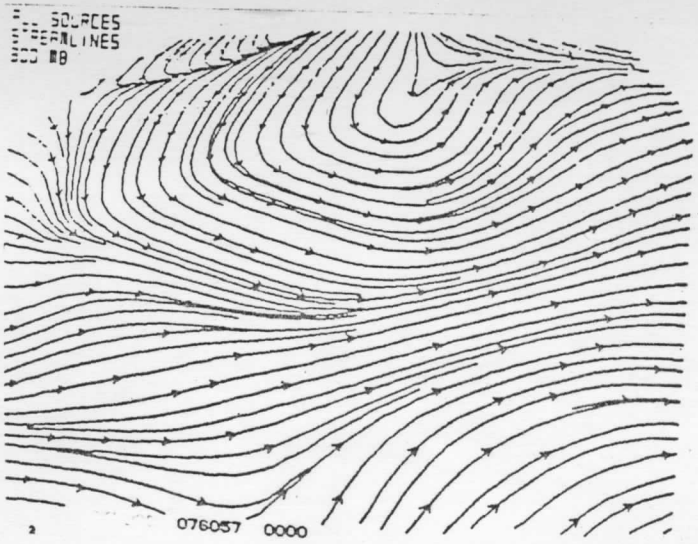

Fig. 43. Streamline analysis of the combined upper level wind set for 26 February 1976

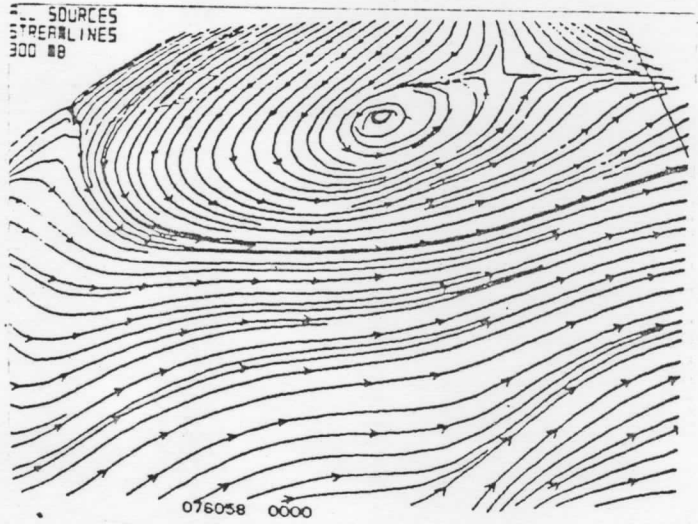

Fig. 44. Streamline analysis of the combined upper level wind set for 27 February 1976

although the wind speed gradient was not as sharply defined. A band of cirrus stretching from west to east marked the location of the jet stream.

By 0000 GMT on February 26 the 300 mb low narrowed its wavelength as a result of the rapid and sharp increase in the amplitude of the high pressure ridge. The center of the storm tracked slightly to the southeast, but the predominant change was in the amplitude of the ridge-trough system.

Aircraft reports for this time period were missing and, therefore, the analysis of the wind field was dependent upon the NESS, SSEC and radiosonde reports. The SSEC wind set was the only source to establish the growth in the amplitude of the ridge. NESS reports were few and could not be analyzed separately. They were used in the combined data set to fill in gaps in the coverage. The combined analysis (fig. 43) marked a 5° southerly shift in the cirrus band. The movement of the polar front was easily identified from the position of the cirrus band.

In the final day of the third event the NMC 300 mb height analysis displayed a very strong, high amplitude ridge in the mid-Pacific. The ridge had amplified so much that it resembled an Omega high. The Gulf of Alaskan low continued to move southward contributing to the amplitude of the ridge. The combined McIDAS analysis relied heavily on the SSEC and aircraft observations (fig. 44). These two sources consistently displayed the movement of the polar front. The aircraft reports were the only ones to establish both the sharp ridge to the west and the deep low in the Gulf. The satellite vectors identified the ridge by cloud motions around the high but failed to properly identify the cyclonic flow of the low in the northern latitudes.

The lower level analysis for the three day period was primarily produced by SSEC and RAOBs. NESS could not consistently produce enough vectors

to allow a proper analysis. The large cyclone influenced the low level flow throughout the entire northern half of the target area. Only in the southern section was the flow anticyclonic. The low migrated slowly eastward during the three days but still remained the dominating force in the streamline pattern. SSEC was able to pick up enough cloud tracers to establish a cyclonic center in the Gulf. This was one of the few times the satellite wind operators were able to distinguish enough cloud tracers to establish a distinct closed cyclonic circulation above 50°N. In general the radiosondes were the sole source to depend on in this region.

The three synoptic events provided a variety of weather features and structures to be analyzed. There were broad slow moving troughs and fast moving short waves, subtropical storms and extra-tropical cyclones. There was the amplification and dissipation of large sub-tropical high pressure systems. These different synoptic formations provided ample data for the comparison of satellite, radiosonde and aircraft reports over the Pacific Ocean.

6. Statistics

The four individual data sources were compared against each other to determine the accuracy of the different wind sets. Two individual wind sets were compared for statistical compatability. A single observation from data source A would search a 200 km horizontal radius and a 200 mb vertical radius for another wind vector from data source B. If a vector from set B fell within the bounds of the search radius from set A a match was made. The wind speed and directions were compared and the differences were computed. Table 1 presents the u and v differences for the data source comparisons during the three synoptic case events. The column labeled matches indicates the number of vectors from the wind set B that

Table 1

Average Absolute Differences for the u and v Components

	Lower Level			Upper Level		
Comparisons	Matches	u-diff.	v-diff.	Matches	u-diff.	v-diff.
SSEC vs SSEC	1129	.2	.3	1819	.2	.5
NESS vs SSEC	582	1.7	1.2	879	3.1	3.6
RAOB vs SSEC	35	1.8	2.4	420	6.6	4.0
Aircraft vs SSEC	--	--	--	591	5.4	2.6
Aircraft vs NESS	--	--	--	222	4.7	4.6
Aircraft vs RAOB	--	--	--	54	4.8	2.5
RAOB vs NESS	0	--	--	0	--	--

fell with the search radius of wind set A.

A cumulative frequency diagram was drawn for the comparisons of the data sources. The cumulative frequency represents the percentage of matches which fell within a given vector magnitude difference. A curve, which has a very steep positive slope and rises rapidily, indicates a close correlation between the two data sets. The steeper the curve rises, the larger the percentage of observations within a given vector magnitude difference. Figure 45 displays the cumulative frequency curves for the upper level winds for all three synoptic events. The highest curve is the comparison of SSEC winds against themselves. Sixty-four percent of the matches fell within a 5 m s^{-1} difference in wind speed. The percentage grows to 87% for a 10 m s^{-1} threshold. The steepness of this curve is expected since an intercomparison of a data set should match up well.

The next curve is the SSEC vs NESS curve. This comparison is quite similar to the intercomparison of the SSEC wind set. Forty-three percent of the matches fell within the 5 m s^{-1} threshold, while 78% fell within 10 m s^{-1}. The similarity in the two curves reveals the compatability between the two sets of satellite derived winds. Many of the SSEC and NESS wind vectors were obtained from the same location since both sources required clouds to obtain the wind vectors.

The next two curves are the aircraft vs SSEC and the aircraft vs NESS. Both of these curves represent a satellite vs aircraft comparison. These two curves have lower cumulative frequencies because of the differences in data gathering procedures. Unlike satellite winds, aircraft winds may be retrieved from cloudy or clear regions. Therefore, a comparison between two different types of data sources would be expected to have lower cumulative frequency curves than a comparison between like sources.

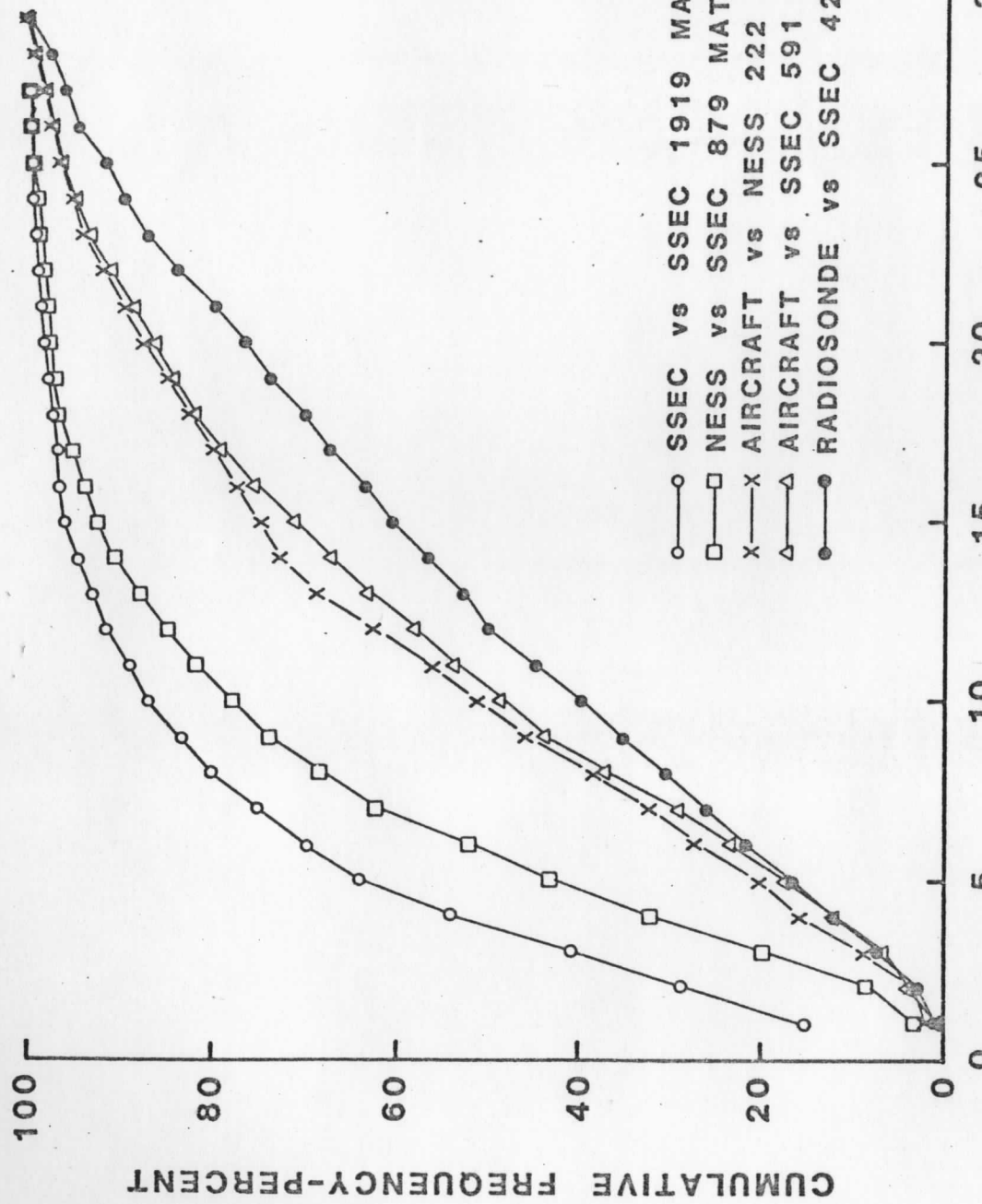

Fig. 45. Cumulative Frequency curves for DST-6

The radiosonde vs SSEC curve is the last curve on the graph. Only 40% of the cumulative frequency is within 10 m s^{-1}, and 61% is explained within the 15 m s^{-1} threshold. A previous FGGE report (Mosher 1980) compared METEOSAT, GOES East and West, and GMS-1 satellite reports with radiosonde observations. The cumulative frequency curves for those comparisons were very similar to the DST-6 satellite vs radiosonde comparisons (fig. 46).

Certainly one reason for the larger vector magnitude difference was the location of the radiosonde reports relative to the SSEC reports. Many of the radiosonde reports were located north of the SSEC wind vectors. The SSEC cloud drift vectors near the limb of the globe suffered from distortions from the curvature of the earth. Therefore, those wind vectors obtained from the northern most latitudes were subject to larger tracking errors. For this reason few satellite winds were obtained in the area north of 50°N. The result was a comparison of northern radiosonde observations with those satellite reports which fell within the 200 km radius. Many of the satellite winds were at the extreme portion of the search radius and, therefore, were subject to larger vector magnitude differences.

Another reason for the discrepancies between radiosonde and satellite reports lies with the height level of the wind vector. The height assignments of satellite winds are restricted by the atmospheric soundings. This results in many vectors being assigned to the same level. Radiosondes on the other hand transmit observations from many levels. The satellite vs radiosonde comparisons may match two vectors assigned to two different heights. Strong vertical shears, especially in the upper atmosphere, could then lead to statistical differences.

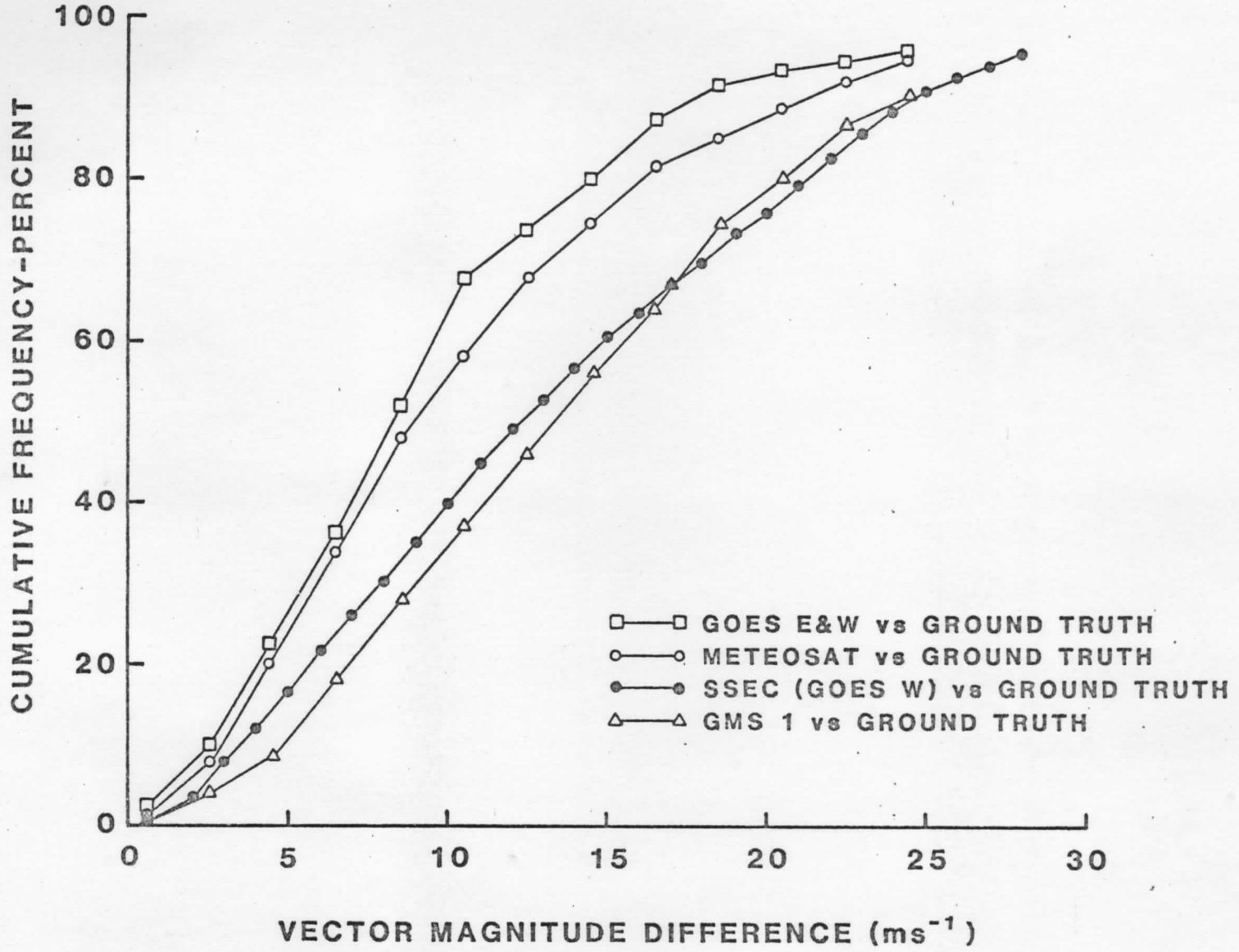

Fig. 46. Comparison of satellite vs radiosonde observations. The solid circle curve is the same as in Figure 45

The other upper level comparisons (aircraft vs radiosondes, and radiosondes vs NESS) produced very few matches and, thus, the curves were not statistically valid. Low level matches were also scarce due to a combination of fewer vectors and large spatial differences. The only low level sources which produced a sufficient number of matches were the NESS vs SSEC satellite comparisons. The low level satellite comparison curve resembled the upper level curve except it was 20% higher. This steeper curve was a result of reduced wind speeds and, thus, smaller vector magnitude differences.

Sampling bias is inherent in a study of this nature. Sources of data are gathered in many different manners by different instruments. Radiosondes have generally been accepted as ground truth over land regions. In the target area chosen for DST-6 the radiosondes could not cover a major portion of the study region and, therefore, were limited in their scope. The near absence of radiosondes in the Pacific led to many erroneous analyses. The target area was too large to permit an accurate extrapolation or interpolation of the data.

The satellite wind vectors by NESS and SSEC are biased towards cloud covered regions. Since the satellite winds are obtained by cloud drift observations, a vector cannot be obtained from a cloud free environment. Clearly this effects any wind field analysis either over land or water. High pressure systems can be identified by cloud flow around them, but the wind field within the subsidence region may be difficult to obtain.

Another major source of bias in satellite data is the height assignment. A cloud drift vector can be categorized into only a few different height levels. These levels are based upon the bottom and/or the top of the cloud. Clouds with bases below 850 mb but above 950 mb had the wind vector placed at the cloud base. If the base was below 950 mb then the wind was assigned

the 950 mb height. Likewise if the cloud top was above 300 mb the cloud vector was assigned to cloud top level. Further sampling biases occurred in middle level height assignments where even more approximations were made.

A third source of satellite bias lives in navigation errors. Navigation used in this manner is the assignment of earth landmarks to the satellite image for alignment and identification of the location of the image. An improper landmark assignment can cause a systematic shift in the cloud drift winds. The navigation used in DST-6 appeared to be quite good and no shift was noted in the data analysis.

7. Conclusions

Satellite winds have been examined carefully for their accuracy and validity. The DST programs established a vehicle for which comparisons between the satellite wind sets and the standard (aircraft and radiosonde) wind sets could be made. In addition, the DST program allowed and encouraged the development of new computer hardware and software which enhanced the capabilities of satellite image retrieval, storage and display systems. Many of the McIDAS features were a direct result of the requirements of the DST program.

The satellite wind sets analyzed in the DST-6 program revealed the capabilities and limits of the current satellite "wind getting" procedures. Cloud drift winds are an important source of wind data in the data sparse region of the world. They identified and located the position and growth of both high and low pressure systems. There are a number of advantages and disadvantages with satellite derived cloud drift winds. The foremost disadvantages are 1) the inability to recover wind vectors from the northern (above 50°) latitudes; 2) there is a limited number of levels from which

wind vectors may be obtained; 3) they are restricted to areas with cloud coverage.

The first disadvantage was readily apparent throughout the DST-6 analysis. Again and again the SSEC and NESS observations failed to adequately describe the wind field over Alaska. The distortion of the images due to the limb effect near the border of the global disk prevented the operators from recovering sufficient winds to describe the wind field.

The second drawback is not as serious as the first. The satellite observations were grouped into low, middle, and upper levels. Streamline and isotachs were produced from middle level observations, although the analysis wasn't presented in this report. The mid-level satellite reports were to few to cover the target area. In many locations the middle level clouds were obscured by upper level cirrus or were very difficult to discern.

The final disadvantage of satellite tracked winds is currently being investigated through the use of the GOES-4 water vapor channel (7.261μ). Since water vapor is present in the atmosphere irregardless of cloud coverage, satellite winds are now possible in the cloud free regions. Early studies indicate a viable data set can be obtained from tracking water vapor features.

Despite the above disadvantages the satellite winds proved to be an excellent source for synoptic wind data. The low level analyses over the oceanic regions were produced almost entirely from satellite winds. The radiosondes were restricted to the land and aircraft reports were limited to the upper levels where they fly over preselected routes. The SSEC analyses were in general better than the NESS analyses because of a greater number of wind vectors per data set. At best there were only half as many NESS vectors provided for analysis. If NESS could increase their number of vectors per wind set then either satellite group could produce a satisfactory

wind field.

The most outstanding feature of this study was the meteorological consistency of the satellite analyses. This was reflected both in the individual satellite wind set and in the combined data set. The progression of the upper and lower level cyclones across the north Pacific was easily identifiable from the cloud vector winds. The jet cores associated with the polar front were also located and tracked as they migrated eastward around the upper level cyclones. The satellite derived wind speeds were, for the most part, in accord with the aircraft reports. Although the satellite produced isotach maxima was not as sharply delineated as the aircraft analyses. The isotach analyses not only pinpointed the jet core, but just as importantly they located the relative minimums within the wind field. In addition, the divergence and relative vorticity fields (not formerly presented in this report) aided in establishing the validity of the synoptic analyses. The overall result was a wind field analysis which confirmed the NMC level III analysis.

The satellite observations provided a valuable means for obtaining wind vectors from remote regions. They complimented and enhanced the radiosonde and aircraft wind sets. Together all four wind sets produced an excellent synoptic analyses. The satellite derived wind vectors are not a replacement for radiosonde or aircraft observations. Rather they are an addition to the data bank of world wide wind reports.

References

Chatters, G. C., and V. E. Suomi, 1975: The Applications of McIDAS, IEEE Transactions Geosci. Electronics, GE-13(3), 136-146.

Mosher, F. R., 1975: Report on the Wisconsin Participating in the August-September 1975 DST Internal Report, Space Science and Engineering Center, Univ. of Wisconsin, Madison, WI.

Mosher, F. R., 1976: Report on the Wisconsin Participation in the January-February 1976 DST, Internal Report, Space Science and Engineering Center, Univ. of Wisconsin, Madison, WI.

Young, M. T., 1975: The GOES Wind Operation, Central Processing and Analysis of Geostationary Satellite Data, NOAA Technical Memorandum NESS 64, 111-121.